bioRxiv preprint doi: https://doi.org/10.1101/2025.11.17.688782; this version posted November 17, 2025. The copyright holder for this preprint (which was not certified by peer review) is the author/funder, who has granted bioRxiv a license to display the preprint in perpetuity. It is made available under aCC-BY 4.0 International license.

Active vision modulates early cortical stages of visual processing: Evidence from MEG and eye-tracking

Christoph Huber-Huber[1,2], Floris P. De Lange[2,3]

[1] Center for Mind/Brain Sciences (CIMeC), University of Trento, Italy

[2] Radboud University, Donders Institute for Brain, Cognition and Behaviour, Netherlands

[3] University of Bonn, Transdisciplinary Research Area Life and Health, Center for Artificial Intelligence and Neuroscience, Bonn, Germany

Corresponding author: Christoph Huber-Huber, christoph.huberhuber@unitn.it

bioRxiv preprint doi: https://doi.org/10.1101/2025.11.17.688782; this version posted November 17, 2025. The copyright holder for this preprint (which was not certified by peer review) is the author/funder, who has granted bioRxiv a license to display the preprint in perpetuity. It is made available under aCC-BY 4.0 International license.

Abstract

It has been hypothesized that the visual system anticipates upcoming visual input contingent on the execution of saccadic eye movements. In line with this idea, it has been shown that changes in visual input across saccades elicit stronger post-saccadic fixation-locked neural responses compared to no-change conditions; an effect known as the *preview effect*. In the present study, we demonstrate that this preview effect depends on active vision and cannot be explained by either classical or spatiotopic adaptation. In a gaze-contingent experiment, in which participants were cued to make saccades to object stimuli, we concurrently recorded magnetoencephalography (MEG) and eye-tracking data. The source-localized MEG signal was deconvolved with stimulus onset and eye movement events in order to account for systematic variation in gaze behavior related to the no-change (valid preview) and change (invalid preview) conditions. Crucially, preview effects in the primary visual and in ventral-occipital cortices were markedly larger when participants made saccades compared to replay blocks in which we simulated the visual consequences of saccades absent saccade execution, demonstrating that the preview effect cannot be simply explained by classic adaptation. A further control condition ruled out spatiotopic adaptation. Our results show that early visual cortical areas which are not known to exhibit saccadic remapping neurons still show signs of sequential neural history effects across saccades. Previous research might have overlooked this influence of active vision because of the lack of an invalid preview condition which breaks the correspondence between pre-saccadic extrafoveal and post-saccadic foveal stimulation.

bioRxiv preprint doi: https://doi.org/10.1101/2025.11.17.688782; this version posted November 17, 2025. The copyright holder for this preprint (which was not certified by peer review) is the author/funder, who has granted bioRxiv a license to display the preprint in perpetuity. It is made available under aCC-BY 4.0 International license.

Introduction

Humans make about three to four saccadic eye movements per second in daily life and it has been hypothesized that, across each of these saccades, the visual system predicts upcoming visual input (1–17). This anticipatory process is thought to be based on input from extrafoveal regions of the visual field, the motor command for an eye movement, and learning about the change in visual appearance from pre-saccadic extrafoveal to post-saccadic foveal input (10,17–25). Consistent with this idea, we and others have previously shown that changing a stimulus during the saccade that is directed to that stimulus, aka an *invalid* preview condition, leads to discrimination performance decrements and a larger post-saccadic neural response compared to a no-change, *valid* preview, condition (26–28). This *preview effect* is reminiscent of the preview effect in reading research (29–37) and could be interpreted in terms of neural surprise within a predictive processing framework (7,11,16).

At present, it is, however, unclear how the neural preview effect comes about. Previous research suggests that neurons in V1 and higher up along the ventral visual stream respond largely in the same way to visual input that is brought about by a saccade compared to conditions in which the eyes remain fixed and saccade-like control conditions are achieved through various types of simulated saccade and fixation onsets (38–41). Studies that find differences between simulated and actual saccade conditions (e.g. 42,43) did not always control perfectly for intra-saccadic stimulation (1,44). Consequently, saccade-independent repetition suppression (45,46), visual mismatch responses (47–51), and neural adaptation (52–54) within the visual cortex could well explain the more pronounced post-saccadic response that was observed in invalid compared to valid preview conditions, meaning that the preview effect would be independent from active vision.

In particular two types of adaptation could explain the neural preview effect: first, adaptation of neurons with very large receptive fields, here called classic adaptation (e.g.

bioRxiv preprint doi: https://doi.org/10.1101/2025.11.17.688782; this version posted November 17, 2025. The copyright holder for this preprint (which was not certified by peer review) is the author/funder, who has granted bioRxiv a license to display the preprint in perpetuity. It is made available under aCC-BY 4.0 International license.

52), and second, craniotopic or temporarily-spatiotopic adaptation (6,55) (see also 56). Although strictly retinotopic adaptation can be ruled out a priori because of the different retinal locations of the pre-saccadic peripheral and the post-saccadic foveal stimulus locations, neurons in particular along the ventral visual stream show receptive fields that are large enough to span both pre- and post-saccadic locations in many preview designs. For instance, neurons in the inferotemporal cortex (IT) of macaque monkeys show large variation in receptive field sizes from a few degrees up to 30-40° (57–60). In humans, evidence from population receptive field mapping using fMRI suggests receptive field sizes of 2-12° (61; in particular Figure 6) or 4-8° (62) in lateral occipital and ventral visual areas. Thus, adaptation of neurons with large receptive fields could explain the reduced response for valid compared to invalid previews.

For spatiotopic adaptation, the adaptor and test stimuli have to appear in the same spatiotopic coordinates before and after a saccade and exactly that is the case for pre- and post-saccadic stimuli in preview designs and in ecologically valid contexts. Evidence for spatiotopic adaptation comes primarily from perceptual studies using tilt aftereffects (55) and the neural basis for this effect has been located in ventral visual areas (63) which are close to or even overlap with the above-mentioned visual areas exhibiting very large receptive fields. However, compared to retinotopic adaptation effects, spatiotopic adaptation shows a distinct feature: it needs time, meaning that spatiotopic adaptation increases with increased time in the form of a blank screen between adaptor and test stimuli (55,63,64).

To examine whether the sequential history effects elicited by a trans-saccadic preview could be explained by classic adaptation or spatiotopic adaptation, we conducted a gaze-contingent experiment in which participants made cued saccades to objects in three different blocked viewing conditions while we coregistered magnetoencephalography (MEG) and eye-tracking data. In the *saccade* viewing blocks, participants actively made saccades to an extrafoveally presented object. In the *replay* viewing blocks, participants kept their

bioRxiv preprint doi: https://doi.org/10.1101/2025.11.17.688782; this version posted November 17, 2025. The copyright holder for this preprint (which was not certified by peer review) is the author/funder, who has granted bioRxiv a license to display the preprint in perpetuity. It is made available under aCC-BY 4.0 International license.

gaze fixed at the center of the screen and instead of moving their eyes, the object moved to the center of the screen. This condition mimicked the visual input obtained in the saccade blocks as well as possible without actual saccade execution. If the preview effect was due to adaptation of neurons with very large receptive fields, it should be the same in these replay blocks compared to the saccade blocks, because the same visually responsive neurons would be triggered in both viewing conditions. In order to make the visual input temporally predictable, as it was in the saccade blocks because of the oculomotor efference copy, object motion was always played-back after a fixed delay. The third type of viewing blocks was the same as the saccade blocks, except that we presented a blank screen between the preview and the target onset and called them *blank* blocks. The preview effect should be larger in these blank blocks compared to the saccade blocks, if it resulted from spatiotopic adaptation, because spatiotopic adaptation increases with a blank interval between adaptor and test stimuli (55). Given that perception and visual action in the form of eye movements are tightly intertwined (21,44,65), it would not be surprising if the preview effect could not completely be explained by adaptation but depended on saccade execution.

Our experimental design contains active eye movements or simulated replay equivalents and gaze-contingent trans-saccadic changes which means that one trial contains more than one stimulus onset with potential follow-up saccades and fixations. Each event triggers an MEG-response and to separate these temporally overlapping responses we used temporal deconvolution (66,67,see also 68,69). This method provides the additional advantage of being able to explicitly model any systematic variation in gaze behavior across conditions which we observed in our experiment.

To preview our preview results, we found a more pronounced difference between valid and invalid preview conditions in the saccade blocks than in the replay blocks and no preview effects in the blank blocks in the primary visual (V1) and the ventral occipital (VO) cortex. These results suggest that early visual cortices are more sensitive to pre-saccadic

bioRxiv preprint doi: https://doi.org/10.1101/2025.11.17.688782; this version posted November 17, 2025. The copyright holder for this preprint (which was not certified by peer review) is the author/funder, who has granted bioRxiv a license to display the preprint in perpetuity. It is made available under aCC-BY 4.0 International license.

extrafoveal information when participants make saccades, compared to when the same visual input is provided without making a saccade.

Results

Preview effects in eye movements and behavior necessitate temporal deconvolution of MEG data

To determine whether the neural preview effect could be explained by classic adaptation, spatiotopic adaptation, or active vision, we measured the source-localized MEG signal time-locked to target foveation in three different types of viewing blocks (Figure 1). However, the preview conditions and viewing blocks did not only affect the MEG signal but also the participants' eye movements. In the saccade and blank blocks, where participants made a cued saccade to a pre-saccadic object (valid preview) or phase-scrambled and blurred version of the same object (invalid preview) (Figure 1A, 1C, 1D), the saccade amplitudes were minimally (by 0.22°), but very consistently, greater for valid (8.13°) than for invalid previews (7.91°, $F(1,35) = 39.71$, $p < .001$, Figure 1F). We, therefore, included each trial's saccade amplitude as covariate in the MEG temporal deconvolution model to explicitly capture the effect of saccade amplitudes on the first post-saccadic EEG/MEG component, aka the lambda response (66,67,70–72), because the lambda response extends into the time window of 100-300 ms where preview effects are usually found.

Interestingly, the preview conditions did not only affect saccade amplitudes but also the follow-up gaze behavior after the initial target fixation and, crucially, this effect varied across viewing blocks. With an invalid preview, participants were more likely to make a follow-up saccade than with a valid preview (Figure 1G), but only in the saccade block ($t(35) = 3.11$, $p < .010$). In the replay block, this effect was reversed (interaction $F(1,35) = 11.04$, $p = .002$). In the blank block, the effect was comparable to the saccade condition (interaction $F(1,35) = 0.01$, $p = .912$) considering first the onset of the blank screen. The subsequent target onset did not appear to further modulate follow-up saccades (interaction with

bioRxiv preprint doi: https://doi.org/10.1101/2025.11.17.688782; this version posted November 17, 2025. The copyright holder for this preprint (which was not certified by peer review) is the author/funder, who has granted bioRxiv a license to display the preprint in perpetuity. It is made available under aCC-BY 4.0 International license.

saccade condition, $F(1,35) = 6.44$, $p = .016$, invalid 875 ms, valid 873 ms, $t(35) = 0.14$, $p = .890$). If a follow-up saccade was made, the time until this saccade happened, that is the duration of the first fixation on the target (Figure 1H), showed the opposite pattern in the saccade ($t(35) = 9.56$, $p < .001$) compared to the replay block ($t(35) = 4.21$, $p < .001$, interaction $F(1,35) = 107.99$, $p < .001$). In the blank blocks, there are two first fixation onsets because of the intermediate blank screen, one on the blank screen and one on the target. For the blank screen onset, the timing of follow-up saccades was similar as in the saccade blocks but less extreme (interaction $F(1,35) = 62.50$, $p < .001$). After the onset of the target, which followed the 400-ms blank screen, there was no evidence anymore for an effect of the preview ($t(35) = 0.79$, $p = .436$, interaction with saccade blocks $F(1,35) = 54.77$, $p < .001$). Because of these patterns in eye movements, we included follow-up saccades as additional events in our deconvolution model. This allowed us to separate the MEG response to the initial fixation form the response elicited by follow-up saccades (66,67).

Besides making a saccade (Figure 1B and 1D) the extrafoveally presented objects or watching the replay (Figure 1C), participants had to report in each trial whether the object was tilted left or right (Figure 1). The manual responses in this tilt discrimination task on the target object also showed a behavioral preview effect (Figure 1E). Response times were faster with a valid (471 ms) compared to an invalid (573 ms) preview ($F(1,35) = 116.64$, $p < .001$) and there was no evidence for a modulation by the viewing blocks (both interaction $p > .823$). Some participants, however, showed on average very early response times, even within the time period of a neural preview effect around 200-250 ms (cf. Figure 1E). In order to avoid that these occasionally very early responses could confound our conclusions from the MEG signal, we added manual response as separate events to our temporal deconvolution model. Error rates did not provide any evidence for preview effects or differences between viewing blocks (all $p > .076$).

bioRxiv preprint doi: https://doi.org/10.1101/2025.11.17.688782; this version posted November 17, 2025. The copyright holder for this preprint (which was not certified by peer review) is the author/funder, who has granted bioRxiv a license to display the preprint in perpetuity. It is made available under aCC-BY 4.0 International license.

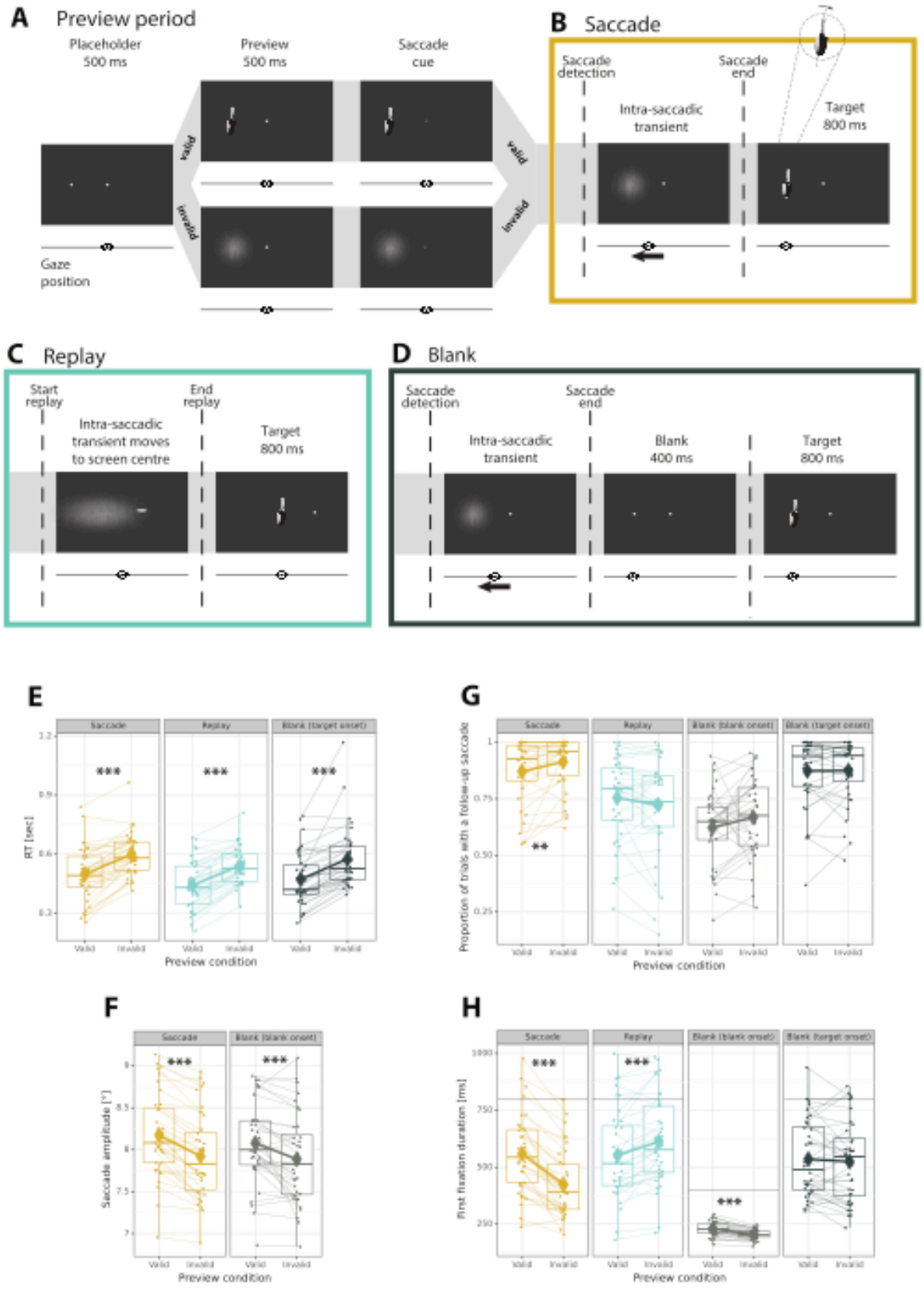

Figure 1. Trial procedure and behavioral results. (A) Stable fixation for 500 ms triggered the presentation of one out of 80 objects, here a garden shovel. In the valid condition, the preview object was the same as the target object; in the invalid condition, the preview was a blurred version of the object. In the saccade blocks (B), the participant made a cued saccade to the preview object which appeared as intact, non-blurred object in both the valid and invalid preview conditions. In the replay blocks (C), the participants maintained stable fixation throughout the trial and the preview object moved into the foveal visual field after a saccadic latency determined per participant depending on their practice trial performance. The blank blocks (D) were the same as the saccade blocks except that a blank screen was presented for 400 ms before the target onset. In all three viewing

bioRxiv preprint doi: https://doi.org/10.1101/2025.11.17.688782; this version posted November 17, 2025. The copyright holder for this preprint (which was not certified by peer review) is the author/funder, who has granted bioRxiv a license to display the preprint in perpetuity. It is made available under aCC-BY 4.0 International license.

conditions, participants reported whether the final target object was tilted left or right. (E) Manual response times showed a significant preview effect in all three viewing conditions. (F) Saccades were significantly larger with valid than with invalid preview for both saccade and blank viewing. (G) In the saccade blocks, the proportion of trials with a follow-up eye movement after the initial target fixation was larger with an invalid compared to with a valid preview. (H) In the saccade blocks, the first fixation on the target (or blank) was longer with a valid than with an invalid preview. This effect was the same for fixations on the blank screen, was reversed for the replay blocks, and was gone after the final target onset in the blank blocks. The black horizontal line indicates target stimulus offsets (800 ms) in all blocks and the end of the blank screen (400 ms) for fixation durations following the blank onset.

The preview effect in the early visual cortex depends on active vision

To test whether the neural preview effect could be explained by adaptation of neurons in with large receptive fields, presumably in mid-to-higher level visual processing, we compared the neural preview effect in an active saccade condition to the neural preview effect in a passive replay condition (Figure 1). We reasoned that having the same visual input in active and passive viewing conditions should trigger the same visually-responsive neurons and therefore the preview effect should be the same in both active and passive viewing conditions only if it resulted from adaptation of visually-responsive neurons.

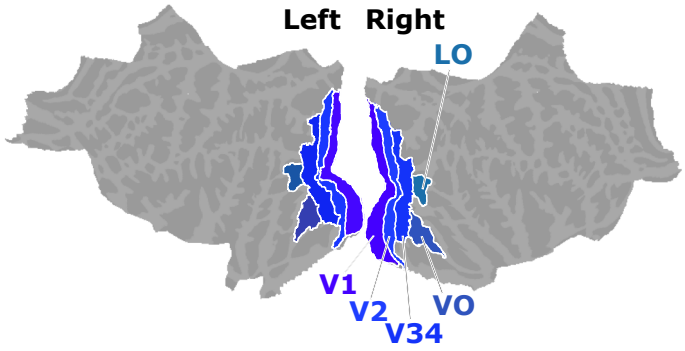

Figure 2. MEG source regions of interest (ROI) based on (73) illustrated on the fsaverage freesurfer brain. We included all visual areas V1, V2, and V3 plus V4 merged into area V34 in order to exhibit a similar number of vertices compared to V1 and V2. In addition, we defined two mid-higher level visual areas: a lateral occipital area (LO) encompassing regions relevant for object processing (74) and a ventral occipital area (VO) with areas associated with spatiotopic adaptation (63). ROIs for the left and right hemispheres were kept separate to capture any lateralized visual activity due to the lateralized preview stimulus. For further details see section Materials and Methods, MEG and eye-tracking data processing, Regions of interest.

We source-localized the MEG signal to five visual cortical surface regions of interest per hemisphere: V1, V2, V34, ventral occipital (VO), and lateral occipital (LO) (Figure 2). Using temporal deconvolution we isolated the MEG response time-locked to foveating the target object at the participant-level (67). For the right-hemisphere ROIs, cluster-based permutation tests at the group level showed a clear preview effect in V1 and in VO after foveating the target object in the saccade blocks (Figure 3A and 3B). In the replay blocks,

bioRxiv preprint doi: https://doi.org/10.1101/2025.11.17.688782; this version posted November 17, 2025. The copyright holder for this preprint (which was not certified by peer review) is the author/funder, who has granted bioRxiv a license to display the preprint in perpetuity. It is made available under aCC-BY 4.0 International license.

there was some evidence for a preview effect only in V1 (Figure 3C and 3D). Crucially, the cluster-based permutation tests of the planned interaction contrast preview (valid, invalid) x viewing block (saccade, replay) indicated that the preview effect was larger, i.e. more negative, in the saccade than in the replay condition in particular in right V1 and right VO around the time period during which preview effects have been observed in the past using EEG, that is around 200 ms after fixation onset (Figure 3G and 3H) (26–28,31). This interaction demonstrates that the preview effect cannot be explained by classic neural adaptation alone. Moreover, within the saccade blocks, the preview-effect cluster appeared numerically before the preview-effect cluster within the replay blocks, which further supports the idea that active vision modulates neural processing in the striate and extrastriate visual cortex.

Note, that in the saccade viewing blocks, the invalid preview showed a more negative source-localized MEG signal than the valid preview condition. This result mimics the direction of the preview effect in the EEG (28,31) suggesting more neural spiking activity in the invalid compared to the valid preview condition.

bioRxiv preprint doi: https://doi.org/10.1101/2025.11.17.688782; this version posted November 17, 2025. The copyright holder for this preprint (which was not certified by peer review) is the author/funder, who has granted bioRxiv a license to display the preprint in perpetuity. It is made available under aCC-BY 4.0 International license.

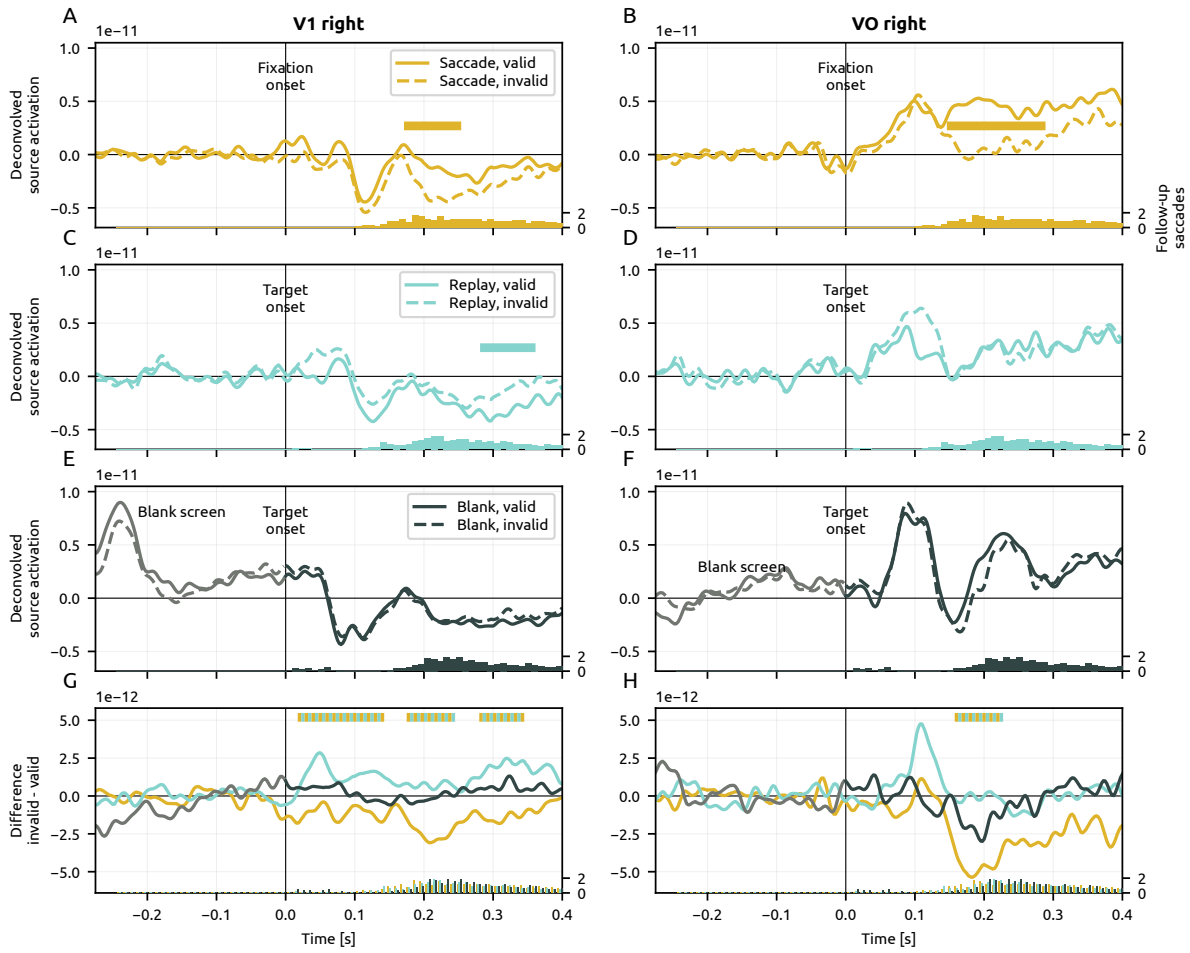

Figure 3. Grand average source-localized and temporally deconvolved MEG signal in the primary visual (V1, left panels) and ventral occipital cortices (VO, right panels) of the right hemisphere. Panels A and B show fixation-locked responses in the valid and invalid preview conditions for the active saccade blocks, panels C and D the target-locked responses for the passive replay, and E and F the target-locked responses for the blocks with the blank screen between preview and target stimuli. Panels G and H compare the preview effect contrast invalid minus valid across the three types of viewing blocks. Horizontal bars indicate significant cluster effects: For both V1 and VO, there was a preview effect in the saccade condition (A and B) which was significantly different from the preview effect in the replay condition (C and D; interaction effect clusters in G and H). The contrast comparing the saccade preview effect to the preview effect in blocks with a blank screen between preview and target stimuli did not show any significant clusters (no corresponding clusters in G and H). The histograms along the x-axis count the number of follow-up saccades per 10 ms time bins, averaged across participants.

Potentially overlapping activity from before the saccade in the replay blocks further supports an active-vision interpretation

Comparing the preview effect in the saccade blocks to the preview effect in the replay blocks showed three significant preview (valid, invalid) x viewing block (saccade, replay) interaction clusters in right V1 which can probably not all be explained by the same process (Figure 3G). Whereas the middle (~200 ms) and later clusters (~300 ms) can be explained by differential responses in V1 time-locked to target foveation, the early cluster

bioRxiv preprint doi: https://doi.org/10.1101/2025.11.17.688782; this version posted November 17, 2025. The copyright holder for this preprint (which was not certified by peer review) is the author/funder, who has granted bioRxiv a license to display the preprint in perpetuity. It is made available under aCC-BY 4.0 International license.

seems to be too early to be related only to the target because it takes some tens of milliseconds for neural activity from the retina to arrive at V1 (75,76). This early effect rather stems from visual input before the saccade, which can be explained as follows: In the saccade blocks, the time interval between preview and target depended gaze-contingently on saccade execution which made the target onset temporally predictable. The replay blocks had a fixed time interval between preview and target in order to make the target onset temporally predictable as well despite the lack of saccades. This fixed preview-to-target interval meant, however, that the neural response to the preview stimulus could not be deconvolved from the neural response to the target stimulus, because deconvolution relies on variation in timing between events (see Methods). As a consequence, the target-locked signal in the replay blocks could in theory still contain overlapping activity from the pre-saccadic preview stimulus (Figure 1A and 1C). Importantly, however, any overlapping activity triggered by the preview stimulus is expected to *exacerbate* target-locked preview effects, but our results show that, even with a potentially exacerbated preview effect in the replay blocks, there is still a difference to the saccade blocks, which further supports our conclusion that classic adaptation cannot explain the preview effect in the early visual cortex.

Spatiotopic adaptation cannot explain the preview effect in early visual cortex

If the preview effect resulted from spatiotopic adaptation, it would become larger as the time between preview (adaptor) and target (test) stimuli increases (63). To investigate that, we added a 400 ms blank screen before the target onset in the blank viewing blocks (Figure 1D). In all other respects the blank viewing blocks were the same as the saccade blocks. We statistically tested whether the blank screen increased the preview effect through the planned preview (valid, invalid) x viewing block (saccade, blank) interaction contrast. This interaction effect did not show any significant clusters in any of the ROIs (all cluster $p > .05$). As can be seen from Figure 3, the preview effects in the blank blocks in right V1 (Figure 3G)

bioRxiv preprint doi: https://doi.org/10.1101/2025.11.17.688782; this version posted November 17, 2025. The copyright holder for this preprint (which was not certified by peer review) is the author/funder, who has granted bioRxiv a license to display the preprint in perpetuity. It is made available under aCC-BY 4.0 International license.

and right VO (Figure 3H) were numerically even smaller than the corresponding significant preview effects in the saccade blocks. We, therefore, conclude that the preview effect can also not be explained by spatiotopic adaptation.

Left V1 shows a complementary signal to right V1

Overall, the evidence for the preview effect was more concentrated in the right hemisphere, which is not completely unexpected. Before saccade onset, the left-lateralized preview stimulus projects to the right hemisphere and the left hemisphere receives input from a uniform screen background. This uniform background is the same for valid and invalid preview conditions, thus, for the left hemisphere there is actually no difference between valid and invalid previews; such a difference exists per design only for the right hemisphere. Although the preview effect is evaluated after the saccade when the object is foveated and processed bilaterally, the pre-saccadic contrast between left and right hemispheres still counts, because the preview effect consists per definition in a match between pre- and post-saccadic visual input. From all ROIs in the left hemisphere, only left V1 showed one significant preview (valid, invalid) x viewing (saccade, replay) interaction cluster very early after fixation/target onset (Figure 4D). This interaction contrast showed the opposite polarity compared to the same very early effect in right V1 (Figure 3G), which suggests that left V1 shows a complementary signal of the same neural source. The preview effects within the saccade blocks and within the replay blocks were not significant in left V1 (Figure 4A and 4B). Regarding the blank blocks, the pattern of results in the left hemisphere was the same as in the right hemisphere. Left V1 did not show any evidence for a modulation of the preview effect by the blank screen compared to the saccade blocks (Figure 4D).

bioRxiv preprint doi: https://doi.org/10.1101/2025.11.17.688782; this version posted November 17, 2025. The copyright holder for this preprint (which was not certified by peer review) is the author/funder, who has granted bioRxiv a license to display the preprint in perpetuity. It is made available under aCC-BY 4.0 International license.

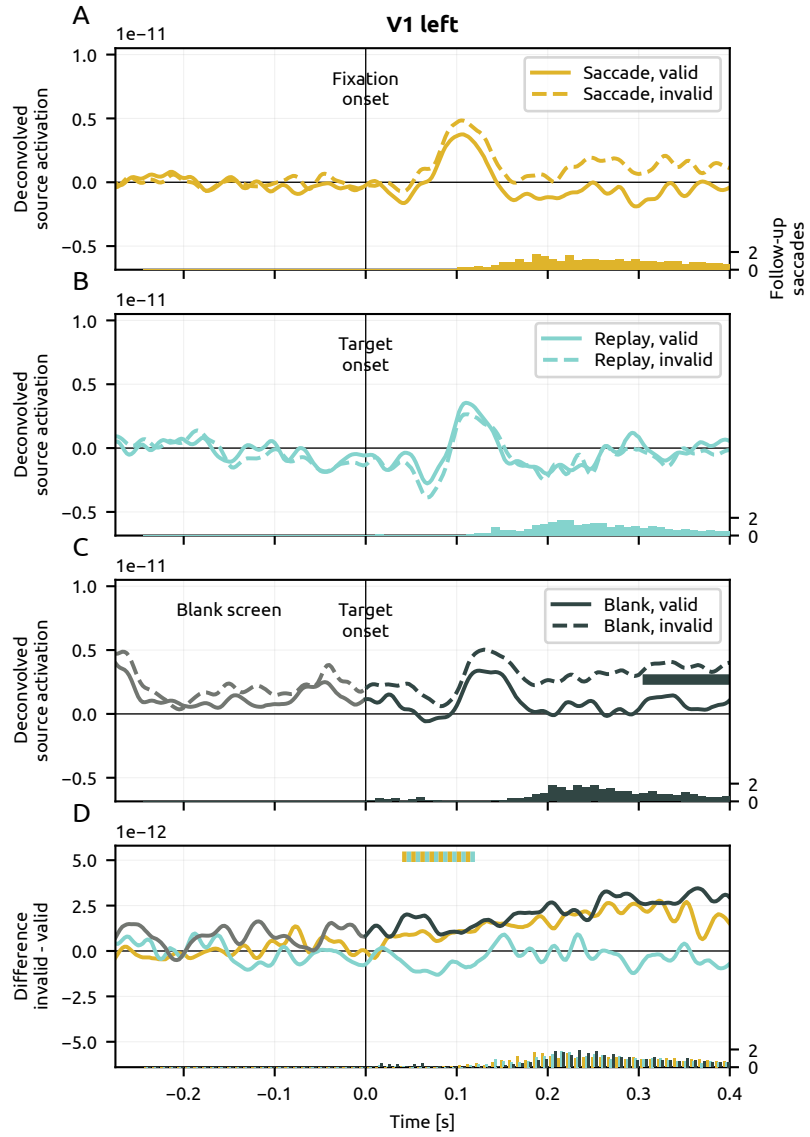

Figure 4. Grand average source-localized and temporally deconvolved MEG signal in the left primary visual cortex (V1). Panel A shows fixation-locked responses in the valid and invalid preview conditions for the active saccade blocks, panel B the target-locked response for the passive replay, and C the target-locked response for the blocks with the blank screen between preview and target stimuli. Panel D compares the preview effect (contrast invalid minus valid) across the three types of viewing blocks. Horizontal bars indicate significant cluster effects: There was one early significant cluster indicating that the preview effect was different between saccade and replay blocks. In contrast, the preview effect in the saccade compared to the blank blocks was not significantly different.

The blank-screen response supports inferences about neural spiking activity from MEG source activations

As can be seen from Figure 3E, in the blank blocks, the target onset was preceded by a very clear and large positive signal across both valid and invalid preview conditions in right V1. This response was obviously triggered by the onset of the blank screen which appeared 400 ms before the target. In general, we baseline-corrected the MEG signal with respect to

bioRxiv preprint doi: https://doi.org/10.1101/2025.11.17.688782; this version posted November 17, 2025. The copyright holder for this preprint (which was not certified by peer review) is the author/funder, who has granted bioRxiv a license to display the preprint in perpetuity. It is made available under aCC-BY 4.0 International license.

the final part of the preview/cue stimulus period in all blocks (Figure 1A, see Methods). Compared to this baseline period, the onset of the blank screen marks an abrupt decrease in visual input which probably leads to a decrease in neuronal spiking activity in early visual cortices. Conversely, a negative deflection in V1 can probably be interpreted as an increase in neuronal firing which matches our interpretation regarding the preview effect in V1 where the more *negative* response in the invalid compared to the valid preview condition is regarded as an *increase* in neuronal spiking activity. Interestingly, the blank screen response was absent in VO (Figure 3F), which suits the general notion that slightly higher visual areas are less affected by sudden low-level visual changes.

Discussion

In the present study, we investigated whether the sequential history effects elicited by a trans-saccadic preview could be explained by classic adaptation of neurons with large receptive fields (52–54) or by craniotopic or transiently-spatiotopic adaptation (55,63) (see also 56) in the visual cortex. For this purpose, participants performed a gaze-contingent task in which they made saccades to extrafoveally presented objects and we compared this active viewing blocks to passive replay blocks where the extrafoveal object moved to the foveal field of view while the participants maintained stable gaze. In the active saccade viewing blocks, we found a robust preview effect in the early visual cortex and this preview effect was significantly smaller in the replay blocks, which demonstrates that the reduced activity in the early visual cortex for a valid preview compared to an invalid preview cannot be explained by adaptation alone; in particular not by adaptation of neurons with receptive fields that are large enough to cover the pre-saccadic extrafoveal and post-saccadic foveal stimulus locations.

To rule out that the preview effect was the result of spatiotopic adaptation, we contrasted the active viewing blocks to a blank control condition in which a blank screen was inserted between the pre-saccadic preview and the post-saccadic target stimulus.

bioRxiv preprint doi: https://doi.org/10.1101/2025.11.17.688782; this version posted November 17, 2025. The copyright holder for this preprint (which was not certified by peer review) is the author/funder, who has granted bioRxiv a license to display the preprint in perpetuity. It is made available under aCC-BY 4.0 International license.

Such a blank screen increases spatiotopic adaptation effects (55,63), but the preview effect in the blank blocks was numerically smaller than the preview effect in the saccade blocks. In sum, our results demonstrate that the preview effect cannot be driven by spatiotopic adaptation and instead depends on the oculomotor and saccade-specific processes implied by active vision.

Previous research has suggested largely similar responses of neurons in V1 and further downstream in ventral visual cortices for stimuli that appear in the visual field because of a saccade compared to saccade-like simulated stimulus onsets (38–41,77). These findings are contrasted by two exceptions (42,43). For these two studies, however, differences between saccade and saccade-like control conditions can in theory be explained by differences in intra-saccadic visual stimulation because of the employed experimental design (1,44,78–80). Intra-saccadic visual stimulation affects the post-saccadic neurophysiological response (81) and can therefore be confounded with an effect from active saccade execution. Apart from this limitation, previous studies on neural responses in visual cortices did not pay much attention to the availability of pre-saccadic preview information which is inherent to active vision (39,82,83). For instance, (39) compared sudden stimulus onsets during fixation to onsets after saccades without corresponding previews. One of these study accounted for the complete dynamics of active vision through a passive replay condition, however, they did not focus on sequential trans-saccadic effect but examined particular types of neural coding principles which did not appear to differ much between active and passive vision conditions (84). Previous research has, thus, not yet been able to provide compelling evidence for the idea that the visual cortex is affected by active vision.

In contrast to the abovementioned studies that found largely similar responses for active saccade and proper passive control conditions, we harnessed a preview effect design with a passive replay control condition and with this setup we could clearly see that active vision modulated the influence of pre-saccadic information on post-saccadic

bioRxiv preprint doi: https://doi.org/10.1101/2025.11.17.688782; this version posted November 17, 2025. The copyright holder for this preprint (which was not certified by peer review) is the author/funder, who has granted bioRxiv a license to display the preprint in perpetuity. It is made available under aCC-BY 4.0 International license.

processing. In particular, the invalid preview condition might have been crucial to reveal this type of trans-saccadic neural history effect because it is the only way that completely breaks the correspondence between pre-saccadic extrafoveal and post-saccadic foveal stimulation. The lack of an invalid preview, or trans-saccadic change, might actually have been the reason why previous studies failed to determine viewing-history effects even in very comprehensive single neuron recordings (e.g. 85). Moreover, our preview effect design has the advantage that any imperfect simulation of visual input in the passive replay condition which could lead to uncontrolled intra-saccadic stimulation (44) cancels out in the valid-invalid contrast.

The same logic of a preview effect design with active and passive viewing conditions has recently been applied by Zhang and colleagues (86) to direct recordings from the macaque superior colliculus with remarkably similar results to ours. In that study, macaques made saccades to gratings that could change their spatial frequency (invalid preview) or remain the same (valid preview) during the saccade. In invalid preview conditions, single neuron and population activity increased after fixation onset but only if the saccade had been actively made and not if the monkey had maintained fixation and the grating had moved from the extrafoveal to the foveal location. Importantly, this effect was recorded from receptive fields that did not overlap the extrafoveal but only the foveal target location which means that these neurons responded to stimuli that they had not been exposed to (86). This remarkably similar result shows that saccade-contingent history effects are not limited to the visual cortex.

Interestingly, using a preview effect design we found trans-saccadic history effects in the primary and ventral visual cortices which are not among the typical brain areas associated with modulations of visual activity by eye-movements. Traditionally, parietal areas, like the lateral intraparietal area (LIP) in monkeys (87), the frontal eye fields (FEF) (88), the superior colliculus (SC), and the mediodorsal thalamus (MD) (89) have been shown to exhibit neurons that change their receptive fields to match the location of upcoming stimuli

bioRxiv preprint doi: https://doi.org/10.1101/2025.11.17.688782; this version posted November 17, 2025. The copyright holder for this preprint (which was not certified by peer review) is the author/funder, who has granted bioRxiv a license to display the preprint in perpetuity. It is made available under aCC-BY 4.0 International license.

in the face of an impending saccade (24,for reviews see 90–98). This phenomenon of predictive remapping has also been reported for earlier visual areas like V2, V3A, and V4 (99–101), is considered to be the basis for perceptual aftereffects across saccades (102–106), and underlies the impression of visual stability despite saccades (20). The idea here is that a copy of the motor signal for a saccade, the efference copy, is sent from the SC via MD to the FEF and further to visual areas in a way that allows to anticipate the visual consequences of the upcoming saccade, i.e. the corollary discharge (107,108), making these visual consequences translucent to subjective experience. However, although being somehow involved in this process, the primary visual cortex and ventral visual areas do not seem to exhibit neurons that show predictive remapping (85,100). Why did we then find a modulation of preview effects by active vision in particular in V1 and ventral occipital cortices?

To us it seems plausible that V1 and ventral occipital areas receive signals about an impending saccade from typical remapping-related areas further downstream, e.g. as close as V2 (99) or further away like LIP or FEF, or from subcortical structures like the SC or MD which leads to a transfer of neural activity that was before the saccade elicited by the extrafoveal stimulus to neurons with foveal receptive fields that cover the post-saccadic target. In other words, although we ruled out classical adaptation and spatiotopic adaptation as possible explanations for the preview effect, it is not impossible that adaptation *in combination with remapping* leads to the reduced post-saccadic activity in valid compared to invalid preview trials that we observed under active vision conditions. Crucially, this type of remapped retinotopic adaptation cannot result from neural fatigue (109), has to act at the timescale of the preview effect around 200 ms after fixation onset, and relies on a surprisingly fast neural activation transfer at the timescale of saccades within tens of milliseconds. Eventually, V1 might contain retinotopic internal model neurons that represent the current environment and which are updated by means of saccade execution and the efference copy to match the newly incoming bottom-up input after saccade offset

bioRxiv preprint doi: https://doi.org/10.1101/2025.11.17.688782; this version posted November 17, 2025. The copyright holder for this preprint (which was not certified by peer review) is the author/funder, who has granted bioRxiv a license to display the preprint in perpetuity. It is made available under aCC-BY 4.0 International license.

(108,110). Interestingly, this type of remapping implies a transfer of information from extrafoveal to foveal cortices which could in theory take place in any experimental context where eye movements are not completely controlled and lead to the presence of extrafoveal visual information in foveal cortical regions (e.g. 111) (see 112 for a perceptual correlate that matchs this proposed neural effect).

Future research could disentangle several ways of how this type of remapping-related adaptation could come about. Neural activity could be transferred across retinotopic neural populations through relays to subcortical structures, through areas further downstream (e.g. 113), or horizontally within the visual hierarchy directly across retinotopic cortices. All three possibilities of how retinotopic neural activity could be transferred across saccades make different predictions in terms of bottom-up and top-down information transfer which implies contrasting predictions regarding laminar activation profiles. Bottom-up connections to pyramidal neurons arrive primarily at supragranular layers (2 and 3) whereas top-down connections arrive at infragranular layers (5 and 6) (114–116). The laminar activation profile in V1 is therefore expected to vary depending on how neural activity is remapped across saccades.

Apart from alterations in bottom-up and top-down processing, the crucial computational principle by which active vision modulates the preview effect could also be of a temporal nature. Temporal expectations are known to enhance effects of expectations (e.g. 117) and one might interpret the preview effect as an effect of expectations with a valid preview entailing an expected target in contrast to an invalid preview entailing an unexpected target. Although we made the target temporally predictable also in the passive replay blocks by including a fixed delay between cue and replay onset, the target might still have been more temporally predictable in the saccade blocks simply because saccade execution directly yields the target onset.

Our finding that active vision affects early cortical stages of visual processing aligns well with a long history of research showing that perception and visual action in the form of

bioRxiv preprint doi: https://doi.org/10.1101/2025.11.17.688782; this version posted November 17, 2025. The copyright holder for this preprint (which was not certified by peer review) is the author/funder, who has granted bioRxiv a license to display the preprint in perpetuity. It is made available under aCC-BY 4.0 International license.

eye movements are tightly intertwined (21,44,65). These ideas date back to academics like (118) and (119) and their conceptual precursors might even be found in the works of medieval and ancient western scholars (cf. 120). Besides these historic ideas, contemporary empirical evidence provides many examples for influences of eye movements on perceptual processing (e.g. 79,80,121) and for the flexible adjustment of these processes according to sensorimotor contingencies (122,123). At the neural level, it is clear that the brain accounts for non-retinal signals of oculomotor origin during eye movements which has recently been elegantly demonstrated in a compelling study in mice showing that the primary visual cortex combines visual and non-visual but eye-movement specific signals of subcortical origin in a way that allows to distinguish sensory input due to self-generated actions, i.e. the reafferent response, from visual motion in the external environment (124) (see also 125–127). In non-human primates, there is evidence that the excitability of neurons in V1 is timed with the perpetual cycle of saccades and fixations showing larger excitability following fixation onsets (128,129) which has been associated with rhythmic and oscillatory neural activity more generally in the context of active sampling (130,131). In addition to these pieces of evidence, we show that active vision leads to trans-saccadic history effects, in terms of neural preview effects, in visual cortices which are not typically associated with saccadic remapping.

Conclusion

The present study highlights the tight link between neural activity in early visual areas and active vision in the form of saccadic eye movements. We demonstrated that the influence of pre-saccadic visual input from extrafoveal regions on post-saccadic processing cannot be explained by classic adaptation or spatiotopic adaptation and instead crucially hinges on saccade execution. Our results suggest that retinotopic neural activity in early visual cortices, in particular in V1 and in ventral-occipital areas, is being transferred from extrafoveal to foveal cortical areas through the execution of saccadic eye movements in

bioRxiv preprint doi: https://doi.org/10.1101/2025.11.17.688782; this version posted November 17, 2025. The copyright holder for this preprint (which was not certified by peer review) is the author/funder, who has granted bioRxiv a license to display the preprint in perpetuity. It is made available under aCC-BY 4.0 International license.

466 combination with an efference copy signal that arrives at V1 and VO either from subcortical
467 or higher-level visual and oculomotor areas. This trans-saccadic updating process suggests
468 that vision unfolds in a profoundly different way, in particular with respect to bottom-up and
469 top-down signaling between early visual cortices and higher-level or subcortical regions,
470 under naturalistic viewing conditions where the visual world is explored with active eye
471 movements in contrast to classic stable-gaze experiments. As a consequence, the growing
472 field of naturalistic neuroscience (132–136) will probably have to focus as much on neural
473 activity as on eye movements and gaze behavior (e.g. 137–139).

bioRxiv preprint doi: https://doi.org/10.1101/2025.11.17.688782; this version posted November 17, 2025. The copyright holder for this preprint (which was not certified by peer review) is the author/funder, who has granted bioRxiv a license to display the preprint in perpetuity. It is made available under aCC-BY 4.0 International license.

Materials and Methods

Participants

Coregistered MEG and eye-tracking data was collected from 39 participants. Written informed consent was obtained from all subjects prior to participating in the study which had been approved by the local ethics committee (CMO region Arnhem/Nijmegen). The data of three participants had to be excluded; for one participant because of problems with the head localization coils, for another because of a magnetic artifact, and for one participant because only a fourth of the whole dataset could have been included for the deconvolution analysis based on the trial exclusion criteria described below.

Stimuli

Eighty objects were selected from the stimulus set of (140), available at https://bradylab.ucsd.edu/stimuli/ObjectsAll.zip, considering that the objects should have horizontal or vertical elements to be useful for the main behavioral task, which was a tilt discrimination task. Additional 10 objects were selected for practice trials. The image background was rendered transparent and, if necessary, the original object orientation was adjusted with the image editor GIMP (https://www.gimp.org) to create an upright view of the object. Images were converted to greyscale with the Python module PIL (https://pypi.org/project/pillow/). Subsequently, mean image luminance across all non-background pixels was reduced to 1/8th of the maximum possible luminance, i.e. pixel value 32 out of 255, and pixel luminance standard deviation was set to 16, with the help of the SHINE toolbox (141).

For each object, we created a phase-scrambled version which served as invalid preview. Note, that we did not maintain the background-foreground distinction for the scramble object, because this would have made the object easier to recognize, but created a two-dimensional gaussian window in the alpha channel that blended the phase-scrambled object with the background and made the object's outline harder to recognize. Finally, the

bioRxiv preprint doi: https://doi.org/10.1101/2025.11.17.688782; this version posted November 17, 2025. The copyright holder for this preprint (which was not certified by peer review) is the author/funder, who has granted bioRxiv a license to display the preprint in perpetuity. It is made available under aCC-BY 4.0 International license.

luminance of the scrambled images was adjusted to the same value as the luminance of the intact images. All image processing code is available with the experiment code (see section Data and code availability).

The objects had a size of 4˚ visual angle and were placed with their center at 8˚ eccentricity to the left of the screen center. Stimulus size and location in visual angels were keep constant across participants by automatically adjusting actual size for each participant individually based on the actually measured screen-eye distance.

A digital light processing (DLP) projector (PROPixx; VPixx Technologies, Saint-Bruno, QC, Canada) rendered the visual stimuli at a refresh rate of 120 Hz on a translucent screen placed 80 cm before the subject. To precisely monitor stimulus onsets, a photodiode was placed in the bottom-right corner of the screen. At that location, a white square was presented with the onset of each stimulus to create a light flash which was recorded via the photodiode into a MISC channel of the MEG system. This procedure revealed the well-known delay of one frame between MEG stimulus onset triggers and the actual change on screen and the time stamps of all stimulus onset triggers events were offline adjusted by the amount of that delay.

Procedure

The temporal sequence of events within a trial was similar to previous gaze-contingent experiments with the preview effect using face images (28,142). In the present study, the experiment consisted of three blocked viewing conditions: a *saccade*, a *replay*, and a *blank* condition (Figure 1). The Participants were informed about which viewing block was coming up at the start of each block. In each of these viewing blocks, a trial started with the presentation of a small fixation dot of 0.1˚ visual angle presented at screen center and an equally sized placeholder dot located at 8˚ eccentricity to the left. Stable gaze at screen center for 500 ms triggered the onset of the preview object which had a maximum diameter of 4° and could be either an intact object (*valid* preview) or its phase-scrambled and

bioRxiv preprint doi: https://doi.org/10.1101/2025.11.17.688782; this version posted November 17, 2025. The copyright holder for this preprint (which was not certified by peer review) is the author/funder, who has granted bioRxiv a license to display the preprint in perpetuity. It is made available under aCC-BY 4.0 International license.

Gaussian-blurred version (*invalid* preview). The preview object was tilted to the left or right by 2°, which was decided randomly in each trial. Stable gaze was defined in terms of the fixation-update events provided online by the Eyelink eye-tracker. A fixation-update event contains the average gaze position across 50 ms of individual gaze samples. If this position was within 2° visual angle from screen center, it counted as stable gaze. If the participants moved their eyes out of this area, the stable-fixation timer restarted. After 500 ms of stable fixation with the preview object on screen, the saccade cue appeared which consisted in the fixation dot turning slightly darker (Figure 1A).

In the saccade blocks (Figure 1B), participants were instructed to monitor the centrally presented dot and as soon as they noticed the saccade cue they had to look at the extrafoveally presented object. The moment at which the eyes started to move was detected online through a heuristic by calculating the difference in screen pixels between two subsequent gaze samples. If this difference was greater than 8 pixels, it counted as a saccade. This threshold value was determined in pilot testing for this specific lab setting. The detected saccade onset triggered a transient image at the target location which was the scrambled and blurred version of a randomly chosen different object. If the eyes had moved too early, i.e. before the saccade cue, the current trial was appended at the end of the program's trial queue and the next trial started. The transient image was presented for one frame only and its purpose was to equalize the amount of visual change between valid and invalid conditions. The transient image was followed by the target object which was always an intact object.

The blank blocks were the same as the saccade blocks, expect that instead of the target object a blank screen containing only the placeholder and fixation dots was presented for 400 ms (Figure 1D). Thus, in this condition, the participants saw a blank screen after the saccade. They were instructed to maintain their gaze at the peripheral placeholder location until the target was presented.

bioRxiv preprint doi: https://doi.org/10.1101/2025.11.17.688782; this version posted November 17, 2025. The copyright holder for this preprint (which was not certified by peer review) is the author/funder, who has granted bioRxiv a license to display the preprint in perpetuity. It is made available under aCC-BY 4.0 International license.

553 The replay blocks were different from the saccade blocks in terms of gaze behavior
554 (Figure 1C). In that condition, participants were instructed to maintain fixation at the screen
555 center throughout the experiment which was controlled by the eye-tracker with the same
556 stable-gaze and saccade detection criteria mentioned above for the saccade blocks. If
557 fixation was too far from screen center or if a saccade was detected, the trial was appended
558 at the end of the trial queue and the next trial started. To match visual input as well as
559 possible to the saccade blocks, the extrafoveal preview object started to move towards the
560 screen center after a fixed time period which was determined for each participant from the
561 saccade latencies that were recorded during the initial practice trials (see below). We call
562 this the *replay* or *replay sequence*. We took the median saccade latency across saccade
563 and blank blocks and subtracted 50 ms to account for the minor speed-up in saccadic
564 latencies that took place throughout the experiment. This adjustment was based on pilot
565 data and previous studies (28,143). The preview object moved in equally spaced steps, one
566 per frame, from the extrafoveal preview location to the screen center. The number of frames
567 for this replay sequence was determined based on how many complete frame durations
568 could fit into a participant's median saccade duration calculated from the practice trial data.
569 The median saccade duration was not adjusted because it does not change much
570 throughout an experiment. The first couple of frames of the replay sequence contained the
571 preview object and only the last frame of the replay sequence contained the transient image
572 to account for the delay between saccade detection and transient presentation in the
573 saccade and blank blocks which also contained only one frame of the transient image. After
574 the replay sequence, the target object was presented at screen center where the
575 participants were still foveating. As in the other viewing blocks, the target object was always
576 intact, that is, not phase scrambled.

577 Introducing a proper replay sequence in the replay blocks was important in order to
578 minimize visual stimulation differences compared to the saccade blocks because, although
579 we are usually not aware of intra-saccadic visual input, the visual system clearly processes

bioRxiv preprint doi: https://doi.org/10.1101/2025.11.17.688782; this version posted November 17, 2025. The copyright holder for this preprint (which was not certified by peer review) is the author/funder, who has granted bioRxiv a license to display the preprint in perpetuity. It is made available under aCC-BY 4.0 International license.

visual input from within a saccadic eye movement (80). However, it is in practice impossible to perfectly mimic the visual input arising from a saccadic eye movement. This would require rotating the whole world around a resting eye. To deal with any remaining differences between saccade and replay blocks, our experiment was designed to cancel out any such remaining differences through the preview effect contrast.

In all three viewing blocks, as soon as the participants had foveate the target object, they had to indicate whether it was tilted left (counter-clockwise) or right (clockwise). The tilt of the post-saccadic target object was 2° and always the same for target and pre-saccadic preview object (illustrated in Figure 1B). In all three viewing blocks, the target object disappeared 800 ms after its onset. Manual responses were given with MEG-compatible button-boxes connected to a DataPixx device (VPixx Technologies, Saint-Bruno, QC, Canada).

Each of the 80 objects appeared once in each condition for each participant. With two preview (valid, invalid) and three types of viewing blocks (saccade, replay, blank), this design resulted in 480 trials which were administered in 15 blocks of 32 trials each. Preview condition trials occurred randomly intermixed within each block. The viewing condition was blocked and the order of blocks was pseudorandom in the sense that before a viewing condition could be repeated both of the other two viewing conditions had to have occurred at least equally often. This constraint was set to balance sequence and practice effects that can result from repeated presentation of the same type of contextual condition in trans-saccadic perception studies (123,cf. 143). Between viewing blocks, participants could take self-paced breaks. If necessary, the experimenter could also halt the experiment during the task, had the participant moved or had the eye-tracker to be recalibrated.

At the start of an experimental session, the participant received a step-by-step explanation of the sequence of event within a trial and they were walked through one trial per viewing block as example. Afterwards they conducted practice trials in each viewing block with the replay condition being the last one in order to obtain the gaze parameters for

bioRxiv preprint doi: https://doi.org/10.1101/2025.11.17.688782; this version posted November 17, 2025. The copyright holder for this preprint (which was not certified by peer review) is the author/funder, who has granted bioRxiv a license to display the preprint in perpetuity. It is made available under aCC-BY 4.0 International license.

the replay sequence from the preceding saccade and blank blocks. During these practice trials, participants received feedback about the correctness of their manual responses in the object tilt discrimination task. If the response was incorrect, the placeholder dot turned red for 300 ms. This feedback was omitted during the experiment proper.

The experiment concluded with one minute of a separate gaze task which had the purpose to obtain MEG data free from task-relevant visual input. This data was added to the training data for the ICA which was conducted to attenuate artifactual eye-movement components primarily related to eyeball motion (see section MEG and eye-tracking data processing and deconvolution analysis, Preprocessing). During this gaze task participants looked back and forth between the fixation dot at screen center and the placeholder dot to the left of fixation. Their gaze was cued by the placeholder and fixation dots alternatingly turning slightly darker in the same way as the saccade cue in the proper experiment.

MEG and eye-tracking data recording and synchronization

MEG data was collected with a 275-channel CTF system with axial gradiometers in an electromagnetically shielded room at a sampling rate of 1200 Hz. Throughout the recording, the participants' head position was monitored online with the help of three positioning coils which had been placed at cardinal landmarks at the nasion, left ear, and right ear according to the standard operating procedure in the lab. If the participant had moved too far away from their starting position, they were verbally guided back into their original position in the break between experimental blocks (144). In addition to MEG data, horizontal and vertical EOG was collected for the first couple of participants in order to rule out gaze data synchronization issues between MEG and eye-tracking computers. After the experimental session, a set of 250 to 300 head shape points was recorded with a motion tracking system. These head shape points served the offline coregistration of the MEG and the MRI coordinate system.

bioRxiv preprint doi: https://doi.org/10.1101/2025.11.17.688782; this version posted November 17, 2025. The copyright holder for this preprint (which was not certified by peer review) is the author/funder, who has granted bioRxiv a license to display the preprint in perpetuity. It is made available under aCC-BY 4.0 International license.

An Eyelink 1000 plus eye-tracker (SR research, Ontario, Canada) recorded eye gaze concurrently to the MEG at a sampling rate of 1000 Hz in the default eye-tracker data file format (SR research's EDF). In addition, the gaze data from the eye-tracker was streamed online via an analog output into dedicated MISC channels of the MEG system. Eye gaze events (fixation start/end, saccade start/end, blink start/end) were provided by the SR research gaze parsing algorithm with a saccade velocity threshold of 35 deg/s and a saccade acceleration threshold of 9500 deg/s^2.

To synchronize MEG and eye-tracking data, trigger events were sent from Psychopy via the python module serial (https://pyserial.readthedocs.io/en/latest/pyserial.html) and a splitter cable connection to the MEG computer and the eye-tracker at the same time. These events were used to offline merge the MEG data with the eye-movement events that had been parsed by the SR research algorithm. The eye-movement events were then used for temporal deconvolution to obtain eye-fixation-locked and stimulus-locked MEG responses.

Anatomical MRI processing

Anatomical T1-weighted MRI data for each participant was either already available at the institute or had been obtained after the MEG experiment with the exception of two participants. For these two participants, it we uses freesurfer's *fsaverage* template brain, skull, and skin meshes warped to the individual participants's head shape points. Apart from using the anatomical templates all other processing steps were the same as for the other participants. The T1 images were automatically segmented and cortical as well as skull and skin surfaces were reconstructed with freesurfer (version 7.4.1, command) and fastsurfer (https://github.com/Deep-MI/FastSurfer).

According to the mne python standard processing pipeline, the outer skin surface model was used to coregister the anatomical MRI data with the MEG sensor locations by matching the locations of the three fiducials (nasion, left, right ear) and the head shape points to the outer skin surface with an Iterative Closest Point (ICP) fitting algorithm.

bioRxiv preprint doi: https://doi.org/10.1101/2025.11.17.688782; this version posted November 17, 2025. The copyright holder for this preprint (which was not certified by peer review) is the author/funder, who has granted bioRxiv a license to display the preprint in perpetuity. It is made available under aCC-BY 4.0 International license.

MEG and eye-tracking data processing and deconvolution analysis

Preprocessing

Both the MEG and eye-tracking data was processed with mne python (version 1.6) (145). The raw MEG signal had been visually inspected for channels with aberrant signals during data collection and any such bad channels were removed and interpolated with spherical spline interpolation during offline data analysis. A third-order gradient compensation was applied to the MEG data before it was filtered with a 0.1 Hz high-pass and a 40 Hz low-pass Hann-windowed finite impulse response filter using mne python's default filter option arguments.

In order to remove heartbeat as well as corneoretinal and myogenic eye and eyeblink artefacts in the MEG signal we ran an independent component analysis (ICA) in a separate pipeline which featured an additional 1 Hz high-pass filter to provide the required largely stationary signal for the ICA. An ICA infomax solution was obtained from all successfully completed trials' data, that is from all trials which had not been aborted because of problems with the trial procedure, and from the separate eye movement task at the end of the experiment. Saccade-related components were automatically labelled by applying the method introduced by (146). In short, if the variance ratio of a component's activation during saccades compared to fixations was larger than 1.1, the component was flagged as saccade related. For most of the participants, visual inspection confirmed the selected components and additionally identified heartbeat components. Three to six components were rejected per participant with the exception of eight components for one participant. The obtained ICA solution weights were then applied to the MEG data in the original pipeline.

In order to integrate the MEG and eye-tracking data in a temporally precise way, the eye-movement events from the Eyelink eye-tracking data file (EDF) were added to the MEG data events array considering the shared experiment triggers which were present in both

bioRxiv preprint doi: https://doi.org/10.1101/2025.11.17.688782; this version posted November 17, 2025. The copyright holder for this preprint (which was not certified by peer review) is the author/funder, who has granted bioRxiv a license to display the preprint in perpetuity. It is made available under aCC-BY 4.0 International license.

eye-tracking and MEG data streams (cf. 30). Following this procedure, we obtained a maximum coregistration error of 2 ms for all common trigger events. After the coregistration with eye-tracking data events, the MEG data was downsampled to 400 Hz.

We ensured that only data from trials where the participants had properly followed the gaze procedure and where the stimulus onsets had happened in time was selected for further processing. In addition, the response time in the speeded object tilt discrimination task had to be within three median absolute deviations per participant and response option (correct, incorrect). In the saccade and blank conditions, the onset of the participant's fixation on the target/blank had to be within 50 ms from target/blank onset and not earlier. In the replay condition, any occasional saccades during the constant fixation period had to be smaller than 3°. There was no eye blink from the stable fixation at trial start up until 500 ms after target onset, including the blank period in the blank blocks.

Source space transformation

The continuous MEG data was transformed into individual participants source spaces with minimum norm estimation (MNE). We used surface source spaces based on the freesurfer white matter segmentation with dipole locations obtained from a recursively subdivided icosahedron downsampled to 5124 locations and a three-layer boundary element model based on the shells between brain, inner skull, outer skull, and outer skin surfaces with default conductivity values of 0.3, 0.006, and 0.3, respectively. Dipole orientations of the source model were restricted to the direction perpendicular to the cortical surface. The noise covariance matrix for the inverse operator was estimated from the different baseline periods that were relevant within a trial. We obtained a noise estimate from the baseline periods with respect to two events per trial that were later relevant for deconvolution: One main event of interest for all three viewing conditions was the onset of the preview object. For the saccade condition, the second event was the onset of the fixation on the target object. For the replay and blank conditions, the second event was the onset of the target object. The baseline period duration was set to the interval of -275 to -

bioRxiv preprint doi: https://doi.org/10.1101/2025.11.17.688782; this version posted November 17, 2025. The copyright holder for this preprint (which was not certified by peer review) is the author/funder, who has granted bioRxiv a license to display the preprint in perpetuity. It is made available under aCC-BY 4.0 International license.

75 ms in order to omit the saccadic spike that was present in the saccade and blank conditions. Correspondingly, from this point on we ran two separate pipelines, one with the noise covariance matrix based on the preview onset event and another one where the noise covariance matrix was based on the fixation/target onset. For each event of interest, we finally report the source space results based on the source space projection with the noise covariance from the baseline period of the respective event. We also ensured that all noise covariance matrices were based on the same number of trials per condition in order to avoid that any condition difference in the source localization could have resulted from imbalances in the number of trials.

Regions of interest (ROI)

After source space projection, the signal was summarized across the vertices of each anatomical region of interest (ROI). Individual participant's regions of interest had been obtained according to the multimodal parcellation of the Human Connectome Project (HCP) (73). The HCP parcellation, which is available for the freesurfer subject *fsaverage*, was transformed to each participant's individual anatomical space using the freesufer mri_label2label function. For each individual ROI, the summary source space signal across vertices was computed by finding the dominant orientation across vertices and flipping the sign of vertex activations to match the dominant orientation (see mne python's *mean_flip* label summary function).

Based on our hypothesis that the preview effect might be explained by different types of adaptation in visual areas, we selected a set of ROIs for statistical analyses from the Glasser atlas (Figure 2). ROIs with considerably smaller numbers of vertices were merged in order to obtain roughly comparable regions. The selected ROIs were: The visual areas *V1* and *V2*. Area V3 merged with V4 to obtain a region called *V34*. The smaller lateral-occipital areas LO1, LO2, LO3 and V4t – V4t is also known as LO2 – merged to form *LO*, because lateral-occipital areas are implicated in object processing and sensory prediction effects (e.g. 74). The ventral occipital areas V8, VMV3, and the ventral visual complex (VVC)

bioRxiv preprint doi: https://doi.org/10.1101/2025.11.17.688782; this version posted November 17, 2025. The copyright holder for this preprint (which was not certified by peer review) is the author/funder, who has granted bioRxiv a license to display the preprint in perpetuity. It is made available under aCC-BY 4.0 International license.

merged to form one region called *VO*, because ventral-occipital cortex is a strong candidate for neurons with large receptive fields (58) and has been identified as a key region for spatiotopic adaptation (63). For further details about the location and differentiation of these areas the reader is referred to the Supplementary Neuroanatomical Results of (73).

Temporal deconvolution

The source activities summarized per region of interest were eventually deconvolved with experiment and eye-movement events using the Unfold.jl toolbox (67) implemented in the Julia programming language (https://julialang.org, version 1.10.0) and access from within python through the juliacall package (version 0.9.15). Temporal deconvolution requires continuous data at the level of single trials. Sections of the continuous data from in between trials or from trials that were not eligible (see preprocessing above) were set to missing data to exclude them from deconvolution.

We used the maximum number of events for deconvolution given our experimental design, considering that only events which vary in their relative timing across trials can be deconvolved. In line with this constraint, we defined as first event of main interest the onset of the preview image in the saccade and blank blocks. For the saccade block, the second event of main interest was the onset of the first fixation on the target. We did not model the preceding saccade onset separately because the time interval from saccade onset to fixation onset was almost constant. In the blank blocks, the next event of interest was the onset of the blank screen. However, the blank screen and the subsequent target onset had a fixed timing which meant that only one of the events could have been selected for the deconvolution. We selected the target onset because our main hypothesis was about the response to the target stimulus. However, the event basis functions were defined for a time range that was long enough to encompass the onset of the preceding blank screen to additionally obtain insights into potential neural omission responses triggered by that screen onset. Similarly, in the replay blocks the onset of the first event of interest, i.e. the preview object, and the onset of the second event of interest, i.e. the onset of the target, occurred at

bioRxiv preprint doi: https://doi.org/10.1101/2025.11.17.688782; this version posted November 17, 2025. The copyright holder for this preprint (which was not certified by peer review) is the author/funder, who has granted bioRxiv a license to display the preprint in perpetuity. It is made available under aCC-BY 4.0 International license.

a fixed timing. This fixed timing served the purpose to render the target temporally predictable because a temporally predictable target was expected to enhance any potential preview effects in this passive replay condition which would make our comparison to the active saccade condition more conservative. For the deconvolution model, this important experimental feature meant that we could only include either the preview onset or the target onset. We opted again for the target onset because the response to the target was of main interest and the deconvolution model was extended in time far enough to encompass the preview onset in order to also compare the neural responses to the preview onsets between all conditions.

Besides the preview onset and the fixation/target onset, we defined four other types of events in the deconvolution model in order to correct for the overlap of their corresponding neural signals: Follow-up saccades after target onsets, additional saccades during the replay sequence which had to be smaller than 3°, additional saccades during presentation of the blank, and the event of the manual response. Participants showed substantial individual variation in the numbers of these three types of additional saccades which happened very likely unintentionally despite the strict gaze-contingent experimental procedure.

The model formulas for each event consisted in the same two predictors preview condition (valid, invalid) and viewing condition (saccade, replay, blank), with the exception of the occasional saccades during the replay sequence and during presentation of the blank screen because these two types of events only occurred within their respective viewing condition and therefore the viewing condition factor was omitted from their model formula. All saccade event formulas and the fixation onset events included saccade amplitude as tenth order spline predictor to account for the non-linear effect of saccade amplitude on the post-saccadic evoked potential (67). To make the replay condition comparable to the saccade condition despite the lack of an actual saccade, we included the simulated

bioRxiv preprint doi: https://doi.org/10.1101/2025.11.17.688782; this version posted November 17, 2025. The copyright holder for this preprint (which was not certified by peer review) is the author/funder, who has granted bioRxiv a license to display the preprint in perpetuity. It is made available under aCC-BY 4.0 International license.

saccade amplitude of 8 dva as continuous predictor for the target onset event in that condition.

All events were modelled with finite impulse response basis functions but the temporal extent of these basis functions, also known as estimation time window length, varied across event types in line with the time point at which an event could occur within a trial, additionally considering that we wanted to capture all possible overlapping responses. The preview onset time window was -275 ms to 2,000 ms after, the fixation/target onset time window was -1,495 ms to 800 ms, for follow-up saccades, saccades during the replay sequence and during blank presentation it was -275 ms to 800 ms, and for the manual response it was -875 ms to 800 ms. The time windows were based on the maximum time intervals between time-varying events across all participants.

The temporal deconvolution was conducted two times, separately for both source space pipelines, for the one with the noise covariance matrix based on the baseline period before preview image onsets and for the one where the noise covariance matrix was based on the period before fixation/target onsets.

The deconvolution analysis was conducted separately for each participant.[1] From the resulting regression coefficients, we calculated the predicted means (using the Julia package *Effects*) per condition, region of interest, and time point. Statistical significance was assessed at the group level by applying cluster-based permutation statistics in the time domain using a significance threshold of p = .05 (147).

Preregistration

This study was preregistered (https://osf.io/uxtqn). We eventually deviated from the preregistration in the sense that we did not go into the source space for individual vertices but selected regions of interest. This step was necessary for computational reasons related to temporal deconvolution. Initially, we did not consider deconvolution for the

[1] We would have preferred to model the data of all participants in one mixed model with random factors for participants and items. This procedure was, however, computationally infeasible, because for only a single data channel the calculations exceeded the maximum resources available on our compute cluster.

bioRxiv preprint doi: https://doi.org/10.1101/2025.11.17.688782; this version posted November 17, 2025. The copyright holder for this preprint (which was not certified by peer review) is the author/funder, who has granted bioRxiv a license to display the preprint in perpetuity. It is made available under aCC-BY 4.0 International license.

preregistration because, based on previous research (28,142), we had assumed to get largely the same types of eye movements in both valid and invalid viewing conditions. However, it turned out that the invalid preview condition with a heavily degraded object eventually led to slightly different saccade characteristics compared to the valid preview condition. To deal with these different characteristics we employed deconvolution which removes the overlapping effect of neural responses to subsequent eye movement events. However, with deconvolution, projecting sensor data into source space becomes less straightforward, because to go into source space with minimum norm estimation we need a noise-covariance matrix which has to be estimated from single-trial data. Per definition we do not have any single-trial data anymore after deconvolution, only the effects aggregated across trials per conditions per participant. Deconvolution is a type of temporally extended regression which means that the result are regression coefficients which summarize the effect across single-trial data. To get source space results with deconvolution, we had to run the deconvolution analysis on data that had already been projected into source space. There are two options of running unfold on source-projected data: Run it for each vertex or run it for ROIs with signal summarized across vertices within one ROI. We chose the second option, because running deconvolution on each vertex would have been computationally infeasible.

Data and code availability

All raw data and the code to generate the results from the raw data can be obtained from the Radboud Data Repository under https://doi.org/10.34973/sqkg-xm80.

bioRxiv preprint doi: https://doi.org/10.1101/2025.11.17.688782; this version posted November 17, 2025. The copyright holder for this preprint (which was not certified by peer review) is the author/funder, who has granted bioRxiv a license to display the preprint in perpetuity. It is made available under aCC-BY 4.0 International license.

Acknowledgements

We thank Robert Oostenveld, Jan-Mathijs Schoffelen, and Britta Westner for insightful comments and suggestions regarding MEG data analysis and Benedikt Ehinger for advice in using Unfold.jl.

This research was supported by a Marie Skłodowska-Curie Individual Fellowship (No. 846392) and by the Italian Ministry of University and Research PNNR NextGenerationEU program (No. 0000027).

References

1. Binda P, Morrone MC. Vision during saccadic eye movements. Annu Rev Vis Sci. 2018;4:193–213.

2. Bosco A, Lappe M, Fattori P. Adaptation of saccades and perceived size after trans-saccadic changes of object size. J Neurosci. 2015;35(43):14448–56.

3. Edwards G, Vetter P, McGruer F, Petro LS, Muckli L. Predictive feedback to V1 dynamically updates with sensory input. Sci Rep. 2017;7(1):1–12.

4. Edwards G, VanRullen R, Cavanagh P. Decoding trans-saccadic memory. J Neurosci. 2018;38(5):1114–23.

5. Fabius JH, Fracasso A, Acunzo DJ, Van der Stigchel S, Melcher D. Low-level visual information is maintained across saccades, allowing for a postsaccadic hand-off between visual areas. J Neurosci [Internet]. 2020 Oct 28; Available from: http://www.jneurosci.org/lookup/doi/10.1523/JNEUROSCI.1169-20.2020

6. Fairhall SL, Schwarzbach J, Lingnau A, Van Koningsbruggen MG, Melcher D. Spatiotopic updating across saccades revealed by spatially-specific fMRI adaptation. NeuroImage. 2017;147(November 2016):339–45.

7. Friston K, Adams RA, Perrinet L, Breakspear M. Perceptions as hypotheses: Saccades as experiments. Front Psychol. 2012;3:1–20.

8. Grzeczkowski L, Deubel H, Szinte M. Stimulus blanking reveals contrast-dependent transsaccadic feature transfer. Sci Rep [Internet]. 2020 Oct 29 [cited 2025 July 11];10(1). Available from: https://www.nature.com/articles/s41598-020-75717-y

9. Grzeczkowski L, van Leeuwen J, Belopolsky AV, Deubel H. Spatiotopic and saccade-specific transsaccadic memory for object detail. J Vis. 2020 July 6;20(7):2.

10. Herwig A, Schneider WX. Predicting object features across saccades: Evidence from object recognition and visual search. J Exp Psychol Gen. 2014;143(5):1903–22.

bioRxiv preprint doi: https://doi.org/10.1101/2025.11.17.688782; this version posted November 17, 2025. The copyright holder for this preprint (which was not certified by peer review) is the author/funder, who has granted bioRxiv a license to display the preprint in perpetuity. It is made available under aCC-BY 4.0 International license.

11. Huber-Huber C, Buonocore A, Melcher D. The extrafoveal preview paradigm as a measure of predictive, active sampling in visual perception. J Vis. 2021 July 20;21(7):12.

12. Hübner C, Schütz AC. A bias in saccadic suppression of shape change. Vision Res. 2021 Sept;186:112–23.

13. Johnston P, Robinson J, Kokkinakis A, Ridgeway S, Simpson M, Johnson S, et al. Temporal and spatial localization of prediction-error signals in the visual brain. Biol Psychol. 2017;125:45–57.

14. Melcher D, Colby CL. Trans-saccadic perception. Trends Cogn Sci. 2008;12:466–73.

15. Parr T, Friston KJ. The active construction of the visual world. Neuropsychologia. 2017;104(July):92–101.

16. Parr T, Friston KJ. Active inference and the anatomy of oculomotion. Neuropsychologia. 2018;111(October 2017):334–43.

17. Valsecchi M, Gegenfurtner KR. Dynamic re-calibration of perceived size in fovea and periphery through predictable size changes. Curr Biol. 2016;26(1):59–63.

18. Bompas A, O'Regan JK. More evidence for sensorimotor adaptation in color perception. J Vis. 2006;6(2):145–53.

19. Bosco A, Rifai K, Wahl S, Fattori P, Lappe M. Trans-saccadic adaptation of perceived size independent of saccadic adaptation. J Vis. 2020;20(7):1–11.

20. Cavanaugh J, Berman RA, Joiner WM, Wurtz RH. Saccadic corollary discharge underlies stable visual perception. J Neurosci. 2016;36:31–42.

21. Herwig A. Linking perception and action by structure or process? Toward an integrative perspective. Neurosci Biobehav Rev. 2015 May;52:105–16.

22. Paeye C, Collins T, Cavanagh P, Herwig A. Calibration of peripheral perception of shape with and without saccadic eye movements. Atten Percept Psychophys. 2018;80(3):723–37.

23. Stewart EEM, Valsecchi M, Schütz AC. A review of interactions between peripheral and foveal vision. J Vis. 2020 Nov 3;20(12):2.

24. Sun LD, Goldberg ME. Corollary discharge and oculomotor proprioception: Cortical mechanisms for spatially accurate vision. Annu Rev Vis Sci. 2016 Oct 14;2(1):61–84.

25. Xie XY, Morrone MC, Burr DC. Serial dependence in orientation judgments at the time of saccades. J Vis. 2023 July 10;23(7):7.

26. Buonocore A, Dimigen O, Melcher D. Post-saccadic face processing is modulated by pre-saccadic preview: Evidence from fixation-related potentials. J Neurosci. 2020 Jan 30;0861–19.

27. de Lissa P, McArthur G, Hawelka S, Palermo R, Mahajan Y, Degno F, et al. Peripheral preview abolishes N170 face-sensitivity at fixation: Using fixation-related potentials to investigate dynamic face processing. Vis Cogn. 2019 Nov 26;27(9–10):740–59.

bioRxiv preprint doi: https://doi.org/10.1101/2025.11.17.688782; this version posted November 17, 2025. The copyright holder for this preprint (which was not certified by peer review) is the author/funder, who has granted bioRxiv a license to display the preprint in perpetuity. It is made available under aCC-BY 4.0 International license.

913 28. Huber-Huber C, Buonocore A, Dimigen O, Hickey C, Melcher D. The peripheral
914 preview effect with faces: Combined EEG and eye-tracking suggests multiple stages of
915 trans-saccadic predictive and non-predictive processing. NeuroImage. 2019;200:344–
916 62.

917 29. Degno F, Loberg O, Zang C, Zhang M, Donnelly N, Liversedge SP. Parafoveal previews
918 and lexical frequency in natural reading: Evidence from eye movements and fixation-
919 related potentials. J Exp Psychol Gen. 2019;148(3):453–74.

920 30. Dimigen O, Sommer W, Hohlfeld A, Jacobs AM, Kliegl R. Coregistration of eye
921 movements and EEG in natural reading: Analyses and review. J Exp Psychol Gen.
922 2011;140:552–72.

923 31. Dimigen O, Kliegl R, Sommer W. Trans-saccadic parafoveal preview benefits in fluent
924 reading: A study with fixation-related brain potentials. NeuroImage. 2012;62:381–93.

925 32. Hutzler F, Braun M, Võ MLH, Engl V, Hofmann M, Dambacher M, et al. Welcome to the
926 real world: Validating fixation-related brain potentials for ecologically valid settings.
927 Brain Res. 2007;1172(1):124–9.

928 33. Kornrumpf B, Niefind F, Sommer W, Dimigen O. Neural correlates of word recognition:
929 A systematic comparison of natural reading and rapid serial visual presentation. J
930 Cogn Neurosci. 2016;28:1374–91.

931 34. Rayner K. The perceptual span and peripheral cues in reading. Cognit Psychol.
932 1975;7:65–81.

933 35. Rayner K. Eye movements in reading and information processing: 20 years of research.
934 Psychol Bull. 1998 Nov;124(3):372–422.

935 36. Schotter ER. Reading ahead by hedging our bets on seeing the future: Eye tracking
936 and electrophysiology evidence for parafoveal lexical processing and saccadic control
937 by partial word recognition. In: Federmeier KD, Watson DG, editors. Current Topics in
938 Language [Internet]. Academic Press; 2018. p. 263–98. Available from:
939 https://doi.org/10.1016/bs.plm.2018.08.011

940 37. Schotter ER, Angele B, Rayner K. Parafoveal processing in reading. Atten Percept
941 Psychophys. 2012;74:5–35.

942 38. Amthor FR, Tootle JS, Gawne TJ. Retinal ganglion cell coding in simulated active
943 vision. Vis Neurosci. 2005 Nov;22(6):789–806.

944 39. DiCarlo JJ, Maunsell JHR. Form representation in monkey inferotemporal cortex is
945 virtually unaltered by free viewing. Nat Neurosci. 2000 Aug;3(8):814–21.

946 40. Gawne TJ, Martin JM. Responses of Primate Visual Cortical Neurons to Stimuli
947 Presented by Flash, Saccade, Blink, and External Darkening. J Neurophysiol. 2002 Nov
948 1;88(5):2178–86.

949 41. Richmond BJ, Hertz JA, Gawne TJ. The relation between V1 neuronal responses and
950 eye movement-like stimulus presentations. Neurocomputing. 1999 June;26–27:247–
951 54.

952 42. MacEvoy SP, Hanks TD, Paradiso MA. Macaque V1 Activity During Natural Vision:
953 Effects of Natural Scenes and Saccades. J Neurophysiol. 2008 Feb;99(2):460–72.

bioRxiv preprint doi: https://doi.org/10.1101/2025.11.17.688782; this version posted November 17, 2025. The copyright holder for this preprint (which was not certified by peer review) is the author/funder, who has granted bioRxiv a license to display the preprint in perpetuity. It is made available under aCC-BY 4.0 International license.

43. McFarland JM, Bondy AG, Saunders RC, Cumming BG, Butts DA. Saccadic modulation of stimulus processing in primary visual cortex. Nat Commun. 2015 Sept 15;6(1):8110.

44. Rolfs M, Schweitzer R. Coupling perception to action through incidental sensory consequences of motor behaviour. Nat Rev Psychol. 2022;1(2):112–23.

45. Grill-Spector K, Henson R, Martin A. Repetition and the brain: Neural models of stimulus-specific effects. Trends Cogn Sci. 2006;10:14–23.

46. Grotheer M, Kovács G. Can predictive coding explain repetition suppression? Cortex. 2016;80:113–24.

47. Czigler I. Visual mismatch negativity: Violation of nonattended environmental regularities. J Psychophysiol. 2007;21:224–30.

48. Garrido MI, Kilner JM, Stephan KE, Friston KJ. The mismatch negativity: A review of underlying mechanisms. Clin Neurophysiol. 2009;120:453–63.

49. Male AG. Predicting the unpredicted … brain response: A systematic review of the feature-related visual mismatch negativity (vMMN) and the experimental parameters that affect it. Bruns P, editor. PLOS ONE. 2025 Feb 27;20(2):e0314415.

50. Pazo-Alvarez P, Cadaveira F, Amenedo E. MMN in the visual modality: A review. Biol Psychol. 2003;63:199–236.

51. Stefanics G, Kremláček J, Czigler I. Visual mismatch negativity: A predictive coding view. Front Hum Neurosci. 2014;8(666):1–19.

52. Benda J. Neural adaptation. Curr Biol. 2021 Feb;31(3):R110–6.

53. Gawne TJ, Woods JM. The responses of visual cortical neurons encode differences across saccades. NeuroReport. 2003;

54. Weber AI, Krishnamurthy K, Fairhall AL. Coding Principles in Adaptation. Annu Rev Vis Sci. 2019 Sept 15;5(1):427–49.

55. Zimmermann E, Morrone MC, Fink GR, Burr D. Spatiotopic neural representations develop slowly across saccades. Curr Biol. 2013;23:R193–4.

56. Cicchini GM, Binda P, Burr DC, Morrone MC. Transient spatiotopic integration across saccadic eye movements mediates visual stability. J Neurophysiol. 2013;109(4):1117–25.

57. De Beeck HO, Vogels R. Spatial sensitivity of macaque inferior temporal neurons. J Comp Neurol. 2000;426(4):505–18.

58. DiCarlo JJ, Zoccolan D, Rust NC. How does the brain solve visual object recognition? Neuron. 2012;73(3):415–34.

59. Ito M, Tamura H, Fujita I, Tanaka K. Size and position invariance of neuronal responses in monkey inferotemporal cortex. J Neurophysiol. 1995;73(1):218–26.

60. Kobatake E, Tanaka K. Neuronal selectivities to complex object features in the ventral visual pathway of the macaque cerebral cortex. J Neurophysiol. 1994;71(3):856–67.

bioRxiv preprint doi: https://doi.org/10.1101/2025.11.17.688782; this version posted November 17, 2025. The copyright holder for this preprint (which was not certified by peer review) is the author/funder, who has granted bioRxiv a license to display the preprint in perpetuity. It is made available under aCC-BY 4.0 International license.

992 61. Amano K, Wandell BA, Dumoulin SO. Visual Field Maps, Population Receptive Field
993 Sizes, and Visual Field Coverage in the Human MT+ Complex. J Neurophysiol. 2009
994 Nov;102(5):2704–18.

995 62. Dumoulin SO, Wandell BA. Population receptive field estimates in human visual cortex.
996 NeuroImage. 2008 Jan 15;39(2):647–60.

997 63. Zimmermann E, Weidner R, Abdollahi RO, Fink GR. Spatiotopic adaptation in visual
998 areas. J Neurosci. 2016;36(37):9526–34.

999 64. Zimmermann E, Weidner R, Fink GR. Spatiotopic updating of visual feature
1000 information. J Vis. 2017;17(12):1–9.

1001 65. Findlay JM, Gilchrist ID. Active Vision [Internet]. Active vision: The psychology of
1002 looking and seeing. Findlay, John M.: U Durham, Dept of Psychology, Ctr for Vision &
1003 Visual Cognition, Durham, United Kingdom: Oxford University Press; 2003. xiii, 220–
1004 xiii, 220 p. Available from:
1005 https://oxford.universitypressscholarship.com/view/10.1093/acprof:oso/978019852479
1006 3.001.0001/acprof-9780198524793

1007 66. Dimigen O, Ehinger BV. Regression-based analysis of combined EEG and eye-tracking
1008 data: Theory and applications. J Vis. 2021 Jan 7;21(1):3.

1009 67. Ehinger BV, Dimigen O. Unfold: an integrated toolbox for overlap correction, non-linear
1010 modeling, and regression-based EEG analysis. PeerJ. 2019;1–33.

1011 68. Smith NJ, Kutas M. Regression-based estimation of ERP waveforms: I. The rERP
1012 framework. Psychophysiology. 2015;52:157–68.

1013 69. Smith NJ, Kutas M. Regression-based estimation of ERP waveforms: II. Nonlinear
1014 effects, overlap correction, and practical considerations. Psychophysiology.
1015 2015;52:169–81.

1016 70. Evans CC. Spontaneous excitation of the visual cortex and association areas —
1017 Lambda waves. Electroencephalogr Clin Neurophysiol. 1953 Feb;5(1):69–74.

1018 71. Kaunitz LN, Kamienkowski JE, Varatharajah A, Sigman M, Quiroga RQ, Ison MJ.
1019 Looking for a face in the crowd: Fixation-related potentials in an eye-movement visual
1020 search task. NeuroImage. 2014;89:297–305.

1021 72. Yagi A. Saccade size and lambda complex in man. Physiol Psychol. 1979;7(4):370–6.

1022 73. Glasser MF, Coalson TS, Robinson EC, Hacker CD, Harwell J, Yacoub E, et al. A multi-
1023 modal parcellation of human cerebral cortex. Nature. 2016;536(7615):171–8.

1024 74. Richter D, Ekman M, de Lange FP. Suppressed sensory response to predictable object
1025 stimuli throughout the ventral visual stream. J Neurosci. 2018;38(34):7452–61.

1026 75. Bullier J. Integrated model of visual processing. Brain Res Rev. 2001 Oct;36(2–3):96–
1027 107.

1028 76. Inui K, Kakigi R. Temporal Analysis of the Flow From V1 to the Extrastriate Cortex in
1029 Humans. J Neurophysiol. 2006 Aug;96(2):775–84.

bioRxiv preprint doi: https://doi.org/10.1101/2025.11.17.688782; this version posted November 17, 2025. The copyright holder for this preprint (which was not certified by peer review) is the author/funder, who has granted bioRxiv a license to display the preprint in perpetuity. It is made available under aCC-BY 4.0 International license.

77. Ruiz O, Paradiso MA. Macaque V1 representations in natural and reduced visual contexts: Spatial and temporal properties and influence of saccadic eye movements. J Neurophysiol. 2012;108(1):324–33.

78. Boi M, Poletti M, Victor JD, Rucci M. Consequences of the Oculomotor Cycle for the Dynamics of Perception. Curr Biol. 2017;27(9):1268–77.

79. Mostofi N, Zhao Z, Intoy J, Boi M, Victor JD, Rucci M. Spatiotemporal Content of Saccade Transients. Curr Biol. 2020;30(20):3999-4008.e2.

80. Schweitzer R, Rolfs M. Intrasaccadic motion streaks jump-start gaze correction. Sci Adv. 2021 July 23;7(30):eabf2218.

81. Nicolas G, Castet E, Rabier A, Kristensen E, Dojat M, Guérin-Dugué A. Neural correlates of intra-saccadic motion perception. J Vis. 2021 Oct 26;21(11):19.

82. Gallant JL, Connor CE, Van Essen DC. Neural activity in areas V1, V2 and V4 during free viewing of natural scenes compared to controlled viewing: NeuroReport. 1998 June;9(9):2153–8.

83. Kagan I, Gur M, Snodderly DM. Saccades and drifts differentially modulate neuronal activity in V1: Effects of retinal image motion, position, and extraretinal influences. J Vis. 2008 Nov 1;8(14):19–19.

84. Vinje WE, Gallant JL. Sparse Coding and Decorrelation in Primary Visual Cortex During Natural Vision. Science. 2000 Feb 18;287(5456):1273–6.

85. Xiao W, Sharma S, Kreiman G, Livingstone MS. Feature-selective responses in macaque visual cortex follow eye movements during natural vision. Nat Neurosci. 2024 Apr 29;1–10.

86. Zhang T, Bogadhi AR, Hafed ZM. Foveal neurons of the monkey superior colliculus signal trans-saccadic prediction errors. Pack C, editor. PLOS Biol. 2025 June 23;23(6):e3003246.

87. Duhamel JR, Colby CL, Goldberg ME. The updating of the representation of visual space in parietal cortex by intended eye movements. Science. 1992;255(5040):90–2.

88. Zirnsak M, Steinmetz N a, Noudoost B, Xu KZ, Moore T. Visual space is compressed in prefrontal cortex before eye movements. Nature. 2014;507(7493):504–7.

89. Sommer MA, Wurtz RH. A Pathway in Primate Brain for Internal Monitoring of Movements. Science. 2002 May 24;296(5572):1480–2.

90. Bisley JW, Mirpour K, Alkan Y. The functional roles of neural remapping in cortex. J Vis. 2020;20(9):6.

91. Burr DC, Morrone MC. Spatiotopic coding and remapping in humans. Philos Trans R Soc B Biol Sci. 2011 Feb 27;366(1564):504–15.

92. Colby CL, Goldberg ME. Space and attention in parietal cortex. Annu Rev Neurosci. 1999 Jan;22:319–49.

93. Golomb JD, Mazer JA. Visual Remapping. Annu Rev Vis Sci. 2021 Sept 15;7(1):257–77.

bioRxiv preprint doi: https://doi.org/10.1101/2025.11.17.688782; this version posted November 17, 2025. The copyright holder for this preprint (which was not certified by peer review) is the author/funder, who has granted bioRxiv a license to display the preprint in perpetuity. It is made available under aCC-BY 4.0 International license.

1068 94. Mathôt S, Theeuwes J. Visual attention and stability. Philos Trans R Soc B Biol Sci.
1069 2011;366:516–27.

1070 95. Neupane S, Guitton D, Pack CC. Perisaccadic remapping: What? How? Why? Rev
1071 Neurosci. 2020 July 28;31(5):505–20.

1072 96. Sommer MA, Wurtz RH. Brain circuits for the internal monitoring of movements. Annu
1073 Rev Neurosci. 2008 July;31:317–38.

1074 97. Wurtz RH, Joiner WM, Berman RA. Neuronal mechanisms for visual stability: Progress
1075 and problems. Philos Trans R Soc B Biol Sci. 2011;366(1564):492–503.

1076 98. Zirnsak M, Moore T. Saccades and shifting receptive fields: Anticipating consequences
1077 or selecting targets? Trends Cogn Sci. 2014;18(12):621–8.

1078 99. Denagamage S, Morton MP, Hudson NV, Nandy AS. Widespread receptive field
1079 remapping in early primate visual cortex. Cell Rep. 2024 Aug 27;43(8):114557.

1080 100. Nakamura K, Colby CL. Updating of the visual representation in monkey striate and
1081 extrastriate cortex during saccades. Proc Natl Acad Sci. 2002 Mar 19;99:4026–31.

1082 101. Neupane S, Guitton D, Pack CC. Two distinct types of remapping in primate cortical
1083 area V4. Nat Commun. 2016;7:10402.

1084 102. He T, Fritsche M, de Lange FP. Predictive remapping of visual features beyond
1085 saccadic targets. J Vis. 2018;18(13):1–16.

1086 103. Mathôt S, Theeuwes J. Evidence for the predictive remapping of visual attention. Exp
1087 Brain Res. 2010;200:117–22.

1088 104. Melcher D. Predictive remapping of visual features precedes saccadic eye movements.
1089 Nat Neurosci. 2007;10:903–7.

1090 105. Rolfs M, Jonikaitis D, Deubel H, Cavanagh P. Predictive remapping of attention across
1091 eye movements. Nat Neurosci. 2011 Feb;14:252–6.

1092 106. Wolfe BA, Whitney D. Saccadic remapping of object-selective information. Atten
1093 Percept Psychophys. 2015;77:2260–9.

1094 107. Cont C, Zimmermann E. The Motor Representation of Sensory Experience. Curr Biol.
1095 2021;31(5):1029-1036.e2.

1096 108. Keller GB, Mrsic-Flogel TD. Predictive Processing: A Canonical Cortical Computation.
1097 Neuron. 2018 Oct;100(2):424–35.

1098 109. Whitmire CJ, Stanley GB. Rapid Sensory Adaptation Redux: A Circuit Perspective.
1099 Neuron. 2016 Oct;92(2):298–315.

1100 110. de Lange FP, Heilbron M, Kok P. How do expectations shape perception? Trends
1101 Cogn Sci. 2018;22:764–79.

1102 111. Williams MA, Baker CI, Op De Beeck HP, Mok Shim W, Dang S, Triantafyllou C, et al.
1103 Feedback of visual object information to foveal retinotopic cortex. Nat Neurosci.
1104 2008;11:1439–45.

bioRxiv preprint doi: https://doi.org/10.1101/2025.11.17.688782; this version posted November 17, 2025. The copyright holder for this preprint (which was not certified by peer review) is the author/funder, who has granted bioRxiv a license to display the preprint in perpetuity. It is made available under aCC-BY 4.0 International license.

112. Kroell LM, Rolfs M. Foveal vision anticipates defining features of eye movement targets. eLife [Internet]. 2022 Sept 9;11. Available from: https://elifesciences.org/articles/78106

113. Khayat PS, Spekreijse H, Roelfsema PR. Correlates of transsaccadic integration in the primary visual cortex of the monkey. Proc Natl Acad Sci. 2004 Aug 24;101(34):12712–7.

114. Bastos AM, Usrey WM, Adams RA, Mangun GR, Fries P, Friston KJ. Canonical microcircuits for predictive coding. Neuron. 2012;76(4):695–711.

115. Bonaiuto JJ, Meyer SS, Little S, Rossiter H, Callaghan MF, Dick F, et al. Lamina-specific cortical dynamics in human visual and sensorimotor cortices. eLife. 2018;7:1–32.

116. Thomas ER, Haarsma J, Nicholson J, Yon D, Kok P, Press C. Predictions and errors are distinctly represented across V1 layers. Curr Biol. 2024 May;34(10):2265-2271.e4.

117. Nobre A, Correa A, Coull J. The hazards of time. Curr Opin Neurobiol. 2007 Aug;17(4):465–70.

118. von Holst E, Mittelstaedt H. Das Reafferenzprinzip [The reafference principle]. Naturwissenschaften. 1950;37(20):464–76.

119. Helmholtz H von. Handbuch der physiologischen Optik [Handbook of physiological optics]. Leipzig: Voss; 1867.

120. Silva JF, Yrjönsuuri M, editors. Active Perception in the History of Philosophy: From Plato to Modern Philosophy [Internet]. Cham: Springer International Publishing; 2014 [cited 2025 Apr 30]. Available from: https://link.springer.com/10.1007/978-3-319-04361-6

121. Grzeczkowski L, Stein A, Rolfs M. Trans-retinal predictive signals of visual features are precise, saccade-specific and operate over a wide range of spatial frequencies. J Neurophysiol. 2024;

122. Grzeczkowski L, Shi Z, Rolfs M, Deubel H. Perceptual learning across saccades: Feature but not location specific. Proc Natl Acad Sci. 2023 Oct 24;120(43):e2303763120.

123. Scholes C, McGraw PV, Roach NW. Learning to silence saccadic suppression. Proc Natl Acad Sci U S A. 2021;118(6).

124. Miura SK, Scanziani M. Distinguishing externally from saccade-induced motion in visual cortex. Nature. 2022;610(7930):135–42.

125. Kleiser R, Skrandies W. Neural correlates of reafference: evoked brain activity during motion perception and saccadic eye movements. Exp Brain Res. 2000 July 17;133(3):312–20.

126. Purpura KP, Kalik SF, Schiff ND. Analysis of perisaccadic field potentials in the occipitotemporal pathway during active vision. J Neurophysiol. 2003;90(5):3455–78.

127. Troncoso XG, McCamy MB, Jazi AN, Cui J, Otero-Millan J, Macknik SL, et al. V1 neurons respond differently to object motion versus motion from eye movements. Nat

bioRxiv preprint doi: https://doi.org/10.1101/2025.11.17.688782; this version posted November 17, 2025. The copyright holder for this preprint (which was not certified by peer review) is the author/funder, who has granted bioRxiv a license to display the preprint in perpetuity. It is made available under aCC-BY 4.0 International license.

Commun [Internet]. 2015 Sept 15 [cited 2025 July 11];6(1). Available from: https://www.nature.com/articles/ncomms9114

128. Barczak A, Haegens S, Ross DA, McGinnis T, Lakatos P, Schroeder CE. Dynamic Modulation of Cortical Excitability during Visual Active Sensing. Cell Rep. 2019;27(12):3447-3459.e3.

129. Rajkai C, Lakatos P, Chen CM, Pincze Z, Karmos G, Schroeder CE. Transient cortical excitation at the onset of visual fixation. Cereb Cortex. 2008;18(1):200–9.

130. Leszczynski M, Schroeder CE. The Role of Neuronal Oscillations in Visual Active Sensing. Front Integr Neurosci [Internet]. 2019 July 23;13. Available from: https://www.frontiersin.org/article/10.3389/fnint.2019.00032/full

131. Schroeder CE, Wilson DA, Radman T, Scharfman H, Lakatos P. Dynamics of Active Sensing and perceptual selection. Curr Opin Neurobiol. 2010 Apr;20(2):172–6.

132. Hasson U. Uncovering a Timescale Hierarchy by Studying the Brain in a Natural Context. J Neurosci. 2025 Mar 19;45(12):e2368242025.

133. Leopold DA, Park SH. Studying the visual brain in its natural rhythm. NeuroImage. 2020;

134. Nastase SA, Goldstein A, Hasson U. Keep it real: rethinking the primacy of experimental control in cognitive neuroscience. NeuroImage. 2020 Nov 15;222:117254.

135. Singh VP, Li J, Dawson K, Mitchell JF, Miller CT. Active vision in freely moving marmosets using head-mounted eye tracking. Proc Natl Acad Sci. 2025 Feb 11;122(6):e2412954122.

136. Sonkusare S, Breakspear M, Guo C. Naturalistic Stimuli in Neuroscience: Critically Acclaimed. Trends Cogn Sci. 2019 Aug 1;23(8):699–714.

137. Li J, Singh V, Mitchell J, Huk A, Miller C. The role of active vision in the primary visual cortex of freely-moving marmosets. J Vis. 2025 July 15;25(9):2695.

138. Parker P. Neural coding and circuitry of active vision in mice. J Vis. 2025 July 15;25(9):1604.

139. Yates JL, Coop SH, Sarch GH, Wu RJ, Butts DA, Rucci M, et al. Detailed characterization of neural selectivity in free viewing primates. Nat Commun. 2023 June 20;14(1):3656.

140. Brady TF, Konkle T, Alvarez GA, Oliva A. Visual long-term memory has a massive storage capacity for object details. Proc Natl Acad Sci. 2008 Sept 23;105(38):14325–9.

141. Willenbockel V, Sadr J, Fiset D, Horne GO, Gosselin F, Tanaka JW. Controlling low-level image properties: the SHINE toolbox. Behav Res Methods. 2010;42:671–84.

142. Huber-Huber C, Melcher D. Saccade execution increases the preview effect with faces: An EEG and eye-tracking coregistration study. Atten Percept Psychophys [Internet]. 2023; Available from: https://doi.org/10.3758/s13414-023-02802-5

bioRxiv preprint doi: https://doi.org/10.1101/2025.11.17.688782; this version posted November 17, 2025. The copyright holder for this preprint (which was not certified by peer review) is the author/funder, who has granted bioRxiv a license to display the preprint in perpetuity. It is made available under aCC-BY 4.0 International license.

143. Huber-Huber C, Melcher D. The behavioural preview effect with faces is susceptible to statistical regularities: Evidence for predictive processing across the saccade. Sci Rep. 2021 Dec 13;11(1):942.

144. Stolk A, Todorovic A, Schoffelen JM, Oostenveld R. Online and offline tools for head movement compensation in MEG. NeuroImage. 2013 Mar;68:39–48.

145. Gramfort A, Luessi M, Larson E, Engemann DA, Strohmeier D, Brodbeck C, et al. MEG and EEG data analysis with MNE-Python. Front Neurosci. 2013;7(7 DEC):1–13.

146. Plöchl M, Ossandón JP, König P. Combining EEG and eye tracking: Identification, characterization, and correction of eye movement artifacts in electroencephalographic data. Front Hum Neurosci. 2012 Jan;6:278.

147. Maris E, Oostenveld R. Nonparametric statistical testing of EEG- and MEG-data. J Neurosci Methods. 2007;164(1):177–90.